
Quickest change detection with unknown parameters: Constant complexity and near optimality

Firas JARBOUI
 ANEO
 Centre Borelli - ENS Paris-saclay
 firasjarbou@gmail.com

Vianey PERCHET
 Criteo AI Lab
 Crest, ENSAE
 vianney.perchet@normalesup.org

Abstract

We consider the quickest change detection problem where both the parameters of pre- and post- change distributions are unknown, which prevents the use of classical simple hypothesis testing. Without additional assumptions, optimal solutions are not tractable as they rely on some minimax and robust variant of the objective. As a consequence, change points might be detected too late for practical applications (in economics, health care or maintenance for instance). Available constant complexity techniques typically solve a relaxed version of the problem, deeply relying on very specific probability distributions and/or some very precise additional knowledge. We consider a totally different approach that leverages the theoretical asymptotic properties of optimal solutions to derive a new scalable approximate algorithm with near optimal performance that runs in $\mathcal{O}(1)$, adapted to even more complex Markovian settings.

1 Introduction

Quickest Change Detection (QCD) problems arise naturally in settings where a latent state controls observable signals [3]. In biology, it is applied in genomic sequencing [4] and in reliable healthcare monitoring [30]. In industry, it finds application in faulty machinery detection [19, 20] and in leak surveillance [40]. It also has environmental applications such as traffic-related pollutants detection [5].

Any autonomous agent designed to interact with the world and achieve multiple goals must be able to detect relevant changes in the signals it is sensing in order to adapt its behaviour accordingly. This is particularly true for reinforcement learning based agents in multi-task settings as their policy is conditioned to some task parameter [8, 37]. In order for the agent to be truly autonomous, it needs to identify the task at hand according to the environment requirement. For example, a robot built to assist cooks in the kitchen should be able to recognise the task being executed (chopping vegetables, cutting meat, ...) without external help to assist them efficiently. Otherwise, the agent requires a higher intelligence (one of the cooks for instance) to control it (by stating the task to be executed). In the general case, the current task is unknown and has to be identified sequentially from external sensory signals. The agent must track the changes as quickly as possible to adapt to its environment. However, current solutions for the QCD problem when task parameters are unknown, either do not scale linearly or impose restrictive conditions on the setting.

We answer both requirements by constructing a new scalable algorithm with similar performances than optimal solutions. It relies on theoretical results on change detection delay under known parameters, that is used as a lower bound for the delay in the unknown case. This improves parameters estimation and thus improves the change point detection. We consider the case where the data is generated by some Markovian processes as in reinforcement learning. We assess our algorithm performances on synthetic data generated using distributions randomly parameterised with neural networks in order to match the complexity and diversity of real life applications. The complexity and benefits of our

approach are detailed and compared to the existing literature in Section 4 (that is postponed as these comparisons require the formalism and notations introduced in subsequent sections).

2 Quickest Change Detection Problems

The QCD problem is formally defined as follows. Consider a sequence of random observations (X_t) where each X_t belongs to some observation space \mathcal{X} (say, an Euclidean space for simplicity) and is drawn from $f_{\theta_t}(\cdot|X_{t-1})$, where the parameter θ_t belongs to some task parameter space Θ and $\{f_{\theta}, \theta \in \Theta\}$ is a parametric probability distribution family (non trivial, in the sense that all f_{θ} are different). The main idea is that, at almost all stages, $\theta_{t+1} = \theta_t$ but there are some “change points” where those two parameters differ. Let us denote by t_k the different change points and, with a slight abuse of notations, by θ_k the different values of the parameters. Formally, the data generating process is therefore: $X_t \sim \sum_{k=0}^K f_{\theta_k}(\cdot|X_{t-1}) \mathbb{1}_{t_k \leq \cdot < t_{k+1}}(t)$.

The overarching objective is to identify as quickly as possible the change points t_k and the associated parameters θ_k , based on the observations (X_t) . Typical procedures propose to tackle iteratively the simple change point detection problem, and for this reason we will focus mainly on the simpler setting of a single change point, where $K = 2$, $t_0 = 0$, $t_1 = \lambda$ and $t_2 = \infty$, where λ is unknown and must be estimated. For a formal description of the model and the different metrics, we will also assume that the parameters (θ_0, θ_1) are drawn from some distribution \mathcal{F} over Θ . As a consequence, the data generating process we consider is described by the following system of Equations 1:

$$\theta_0, \theta_1 \sim \mathcal{F} \quad \text{and} \quad \begin{cases} X_{t+1} \sim f_{\theta_0}(\cdot|X_t) & \text{if } t \leq \lambda \\ X_{t+1} \sim f_{\theta_1}(\cdot|X_t) & \text{if } t > \lambda \end{cases} . \quad (1)$$

2.1 Criteria definitions

As mentioned before, the objective is to detect change points as quickly as possible while controlling the errors. There exist different metrics to evaluate algorithm performances; they basically all minimise some delay measurements while keeping the rate of type I errors (false positive change detection) under a certain level. Traditionally, there are two antagonistic ways to construct them: the MIN-MAX and the BAYESIAN settings [39].

First, we denote by \mathbb{P}_n (resp. \mathbb{E}_n) the data probability distribution (resp. the expectation) conditioned to the change point happening at $\lambda = n$. This last event happens randomly with some unknown probability $\mu(\cdot)$ over \mathbb{N} – with the notation that bold characters designate random variables –, and we denote by \mathbb{P}^μ (resp. \mathbb{E}^μ) the data probability distribution (resp. the expectation), integrated over μ , i.e., for any event Ω , it holds that $\mathbb{P}^\mu(\Omega) = \sum_n \mu(\lambda = n) \mathbb{P}_n(\Omega)$. In the following, we describe the existing formulations of the QCD problem where the goal is to identify an optimal stopping time τ :

BAYESIAN formulation: In this formulation, the error is the Probability of False Alarms (**PFA**) with respect to \mathbb{P}^μ . The delay is evaluated as the Average Detection Delay (**ADD**) with respect to \mathbb{E}^μ .

$$\mathbf{PFA}(\tau) = \mathbb{P}^\mu(\tau < \lambda) ; \quad \mathbf{ADD}(\tau) = \mathbb{E}^\mu[\tau - \lambda | \tau > \lambda]$$

In this setting, the goal is to minimise **ADD** while keeping **PFA** below a certain level α (as in Shiryaev formulation [31]). Formally, this rewrites into:

$$(\text{SHIRYAEV}) \quad \begin{cases} \nu_\alpha = \operatorname{argmin}_{\tau \in \Delta_\alpha} \mathbf{ADD}(\tau) \\ \Delta_\alpha = \{\tau : \mathbf{PFA}(\tau) < \alpha\} \end{cases} \quad (2)$$

Min-Max formulation: The MIN-MAX formulation disregards prior distribution over the change point. As a consequence, the error is measured as the False Alarm Rate (**FAR**) with respect to the worst case scenario where no change occurs (\mathbb{P}_∞). As for the delay, two possibilities are studied: the Worst Average Detection Delay (**WADD**) and the Conditional Average Detection Delay (**CADD**). **WADD** evaluates this delay with respect to the worst scenario in terms of both the change point and the observations. **CADD** is a less pessimistic evaluation as it only considers the worst scenario in terms of change point. Mathematically they are defined as:

$$\mathbf{FAR}(\tau) = \frac{1}{\mathbb{E}_\infty[\tau]} \quad \text{and} \quad \begin{cases} \mathbf{WADD}(\tau) = \sup_n \operatorname{esssup}_{X^n} \mathbb{E}_n[(\tau - n)^+ | X^n] \\ \mathbf{CADD}(\tau) = \sup_n \mathbb{E}_n[(\tau - n) | \tau > \lambda] \end{cases}$$

where X^n designates all observation up to the n^{th} one. In this setting, the goal is to minimise either **WADD** (Lorden formulation [18]); or **CADD** (Pollak formulation [26]) while keeping **FAR** below a certain level α . Formally, these problems are written as follows:

$$\text{(LORDEN)} \begin{cases} \nu_\alpha = \operatorname{argmin}_{\tau \in \Delta_\alpha} \mathbf{WADD}(\tau) \\ \Delta_\alpha = \{\tau : \mathbf{FAR}(\tau) < \alpha\} \end{cases} ; \text{(POLLAK)} \begin{cases} \nu_\alpha = \operatorname{argmin}_{\tau \in \Delta_\alpha} \mathbf{CADD}(\tau) \\ \Delta_\alpha = \{\tau : \mathbf{FAR}(\tau) < \alpha\} \end{cases} \quad (3)$$

3 Temporal weight redistribution

In this section, we propose to exploit the detection delay of optimal procedures under known parameters (which is by construction a lower bound for the detection delay under unknown parameters) to learn the parameters θ_0^* and θ_1^* . This will naturally lead to some data segmentation used to learn and estimate these parameters. The obtained approximations are then used to perform simple hypothesis testings. In Section 3.1, we provide a reminder of the asymptotic behaviour of optimal solutions under known parameters. In Section 3.2, we introduce formally a proxy formulation to the QCD problem under unknown parameters that can be solved in a tractable manner. Finally we discuss in Section 3.3 the limitations of this approach and provide practical solutions to mitigate them.

3.1 Asymptotic behaviour of the solution to the Bayesian formulation

Under known parameters, optimal solutions for any of the defined QCD problems consist in computing some statistics, denoted by $S_n^{\theta_0, \theta_1}$ along with a threshold B_α . The optimal stopping time ν_α is the first time $S_n^{\theta_0, \theta_1}$ exceeds B_α . We provide a more detailed description in Appendix A.1. The SHIRYAEV algorithm [31] is asymptotically optimal (in the sens of the BAYESIAN formulation) in the non i.i.d. case [36] under the following r -quick convergence¹ assumption:

Hypothesis 1 *Given f_{θ_0} and f_{θ_1} , there exists $q \in \mathbb{R}$ and $r \in \mathbb{N}$ such that for any $k \in \mathbb{N}$:*

$$\frac{1}{n} \sum_{t=k}^{k+n} \frac{f_{\theta_1}(X_{t+1}|X_t)}{f_{\theta_0}(X_{t+1}|X_t)} \xrightarrow[n \rightarrow +\infty]{r\text{-quickly}} q \quad (4)$$

Under Hypothesis 1, and with exponential or heavy tail prior μ , the SHIRYAEV algorithm is asymptotically optimal [36]. In addition, the moments of **ADD** satisfy the following property for all $m \leq r$ [36]:

$$\mathbb{E}^\mu[(\nu_\alpha - \lambda)^m | \tau > \lambda] \stackrel{\alpha \rightarrow 0}{\sim} \mathbb{E}^\mu[(\nu_\alpha^S - \lambda)^m] \stackrel{\alpha \rightarrow 0}{\sim} \left(\frac{|\log(\alpha)|}{q+d} \right)^m \quad (5)$$

where ν_α^S is the SHIRYAEV algorithm's stopping time and $d = -\lim_{n \rightarrow \infty} \log \mathbb{P}(\lambda > n+1)/n$. Our approach to the QCD problem under unknown parameters relies on the asymptotic behaviour from Equation (5) up to the second order ($r = 2$).

3.2 Rational for Temporal Weight redistribution

In the following, we denote the true parameters by θ_0^* and θ_1^* and the corresponding stationary distributions by Π_0^* and Π_1^* (that are well defined for irreducible Markov Chains). The purpose of this section is to devise an algorithm learning the parameters θ_0^* and θ_1^* using the asymptotic behaviour of the detection delay under known parameters. The delay predicted in Equation (5) is a performance lower bound in our setting (otherwise it would contradict the optimality of the SHIRYAEV algorithm). Intuitively, the idea is to learn θ_1^* using the last $\frac{|\log(\alpha)|}{q+d}$ observation and to learn θ_0^* using previous observation. This simple technique happens to be efficient and computationally simple.

Parameters optimisation: The optimal $S_t^{\theta_0, \theta_1}$ – the SHIRYAEV statistic for the BAYESIAN formulation and the CUSUM statistic for the MIN-MAX one – has a specific form (see Equations (13) and (14) in Appendix). Thus, either formulations of the QCD problem is equivalent to:

$$\nu_\alpha = \operatorname{argmin}_t \{t | S_t^{\theta_0, \theta_1} > B_\alpha\} \text{ with } \begin{cases} \theta_0 = \operatorname{argmin}_\theta g_0(\theta, \theta^1) = \operatorname{argmin}_\theta \mathbb{E}_0 \left[\log \frac{f_{\theta^1}(X_{t+1}|X_t)}{f_\theta(X_{t+1}|X_t)} \right] \\ \theta_1 = \operatorname{argmax}_\theta g_1(\theta^0, \theta) = \operatorname{argmin}_\theta \mathbb{E}_1 \left[\log \frac{f_\theta(X_{t+1}|X_t)}{f_{\theta^0}(X_{t+1}|X_t)} \right] \end{cases}, \quad (6)$$

¹A formal reminder on the definition of r -quick convergence is provided in Appendix B for completeness.

where (θ^0, θ^1) are random initialisation parameters, and $\mathbb{E}_{k \in \{0,1\}}$ is the expectation with respect to the probability distribution $\mathbb{P}_k(X_t, X_{t+1}) = \Pi_k^*(X_t) f_{\theta_k^*}(X_{t+1}|X_t)$. In fact, the solution ν_α to Equation (6) is the optimal stopping time under the true parameters. This follows from Lemma 1:

Lemma 1 θ_0^* and θ_1^* verify the following for any θ_0, θ_1 :

$$\theta_0^* = \operatorname{argmin}_\theta g_0(\theta, \theta_1) ; \theta_1^* = \operatorname{argmax}_\theta g_1(\theta_0, \theta) \quad (7)$$

In order to solve the equivalent Bayesian QCD problem of Equation (6) under unknown parameters, a good approximation of the functions g_0 and g_1 given the observations $(X_t)_0^n$ is needed. This requires the ability to distinguish pre-change samples from post-change samples and this is precisely why optimal solutions are intractable. They rely on computing the statistics for any possible change point and then consider the worst case scenario. Previous approximate solutions simplify the setting by using domain knowledge to infer the pre-change distribution and by using a sliding window to evaluate the post-change distribution. The window size w is unfortunately an irreducible delay.

Since the observations are sampled according to f_{θ_0} before the change point λ , the probability that the t^{th} observation is sampled from the pre-change distribution (denoted $X_t \sim f_{\theta_0}$ to alleviate notations) is equal to the probability that the change point happened after t . Reciprocally, the probability that the t^{th} observation is sampled from the post-change distribution ($X_t \sim f_{\theta_1}$) is equal to the probability that the change point happened before t . Conditioned to the optimal stopping time being detected at the n^{th} observation ($\nu_\alpha = n$), these equalities still hold true:

$$\mathbb{P}(X_t \sim f_{\theta_0} | \nu_\alpha = n) = \mathbb{P}(\lambda > t | \nu_\alpha = n) ; \mathbb{P}(X_t \sim f_{\theta_1} | \nu_\alpha = n) = \mathbb{P}(\lambda < t | \nu_\alpha = n) \quad (8)$$

Given the optimal stopping time ν_α , the asymptotic behaviour from Equation (5) provides an approximation to the posterior distribution of the change point $\mathbb{P}(\lambda = t | \nu_\alpha = n)$. The objective of this section is to exploit the posterior change point distribution to construct a family of functions that are good approximations of g_0 and g_1 . Consider the following family of functions:

$$g_0^n(\theta_0, \theta_1) = \mathbb{E}_0^n \left[\log\left(\frac{f_{\theta_1}}{f_{\theta_0}}\right)(X_{\tau+1}|X_\tau) \right] ; g_1^n(\theta_0, \theta_1) = \mathbb{E}_1^n \left[\log\left(\frac{f_{\theta_1}}{f_{\theta_0}}\right)(X_{\tau+1}|X_\tau) \right],$$

where both the observations X_t and the indices τ are the following random variables. The observations are generated using Equation (1) with a finite horizon t_2 and τ is sampled with respect to the following:

$$\begin{aligned} \text{in } \mathbb{E}_0^n : \tau &\sim \mathbb{P}(\lambda > \tau | \nu_\alpha = n) / \sum_{i=0}^{t_2} \mathbb{P}(\lambda > i | \nu_\alpha = n) \\ \text{in } \mathbb{E}_1^n : \tau &\sim \mathbb{P}(\lambda < \tau | \nu_\alpha = n) / \sum_{i=0}^{t_2} \mathbb{P}(\lambda < i | \nu_\alpha = n) \end{aligned}$$

The family of functions g_k^n are a re-weighted expectation of the log-likelihood ratio of the observations using $\mathbb{P}(\lambda | \nu_\alpha = n)$. Basically, we propose to approximate g_0 and g_1 (under the assumption that the Shiryaev optimal detection happens at the n^{th} observation: $\nu_\alpha = n$), by associating to each observation X_τ a weight proportional to $\mathbb{P}(\lambda > \tau | \nu_\alpha = n)$ when estimating g_0 , and respectively with a weight proportional to $\mathbb{P}(\lambda < \tau | \nu_\alpha = n)$ when estimating g_1 . The following Lemma 2 guarantees point-wise convergence of these approximations to g_0 and/or g_1 . In addition, this family of functions is tractable as we can approximate asymptotically $\mathbb{P}(\nu_\alpha = n)$ using the theoretical delay behaviour of the SHIRYAEV algorithms presented in Equation (5).

Lemma 2 For any given parameters (θ_0, θ_1) , the following convergences hold:

$$\text{If } \lambda = \infty, \text{ then: } \lim_{n, t_2 \rightarrow \infty} |g_0^n(\theta_0, \theta_1) - g_0(\theta_0, \theta_1)| = \lim_{n, t_2 \rightarrow \infty} |g_1^n(\theta_0, \theta_1) - g_0(\theta_0, \theta_1)| = 0$$

$$\text{If } \lambda < \infty, \text{ then: } \begin{cases} \lim_{n, t_2 \rightarrow \infty} |g_0^n(\theta_0, \theta_1) - g_1(\theta_0, \theta_1)| &= 0 \\ \lim_{n, t_2 \rightarrow \infty} |g_1^n(\theta_0, \theta_1) - g_1(\theta_0, \theta_1)| &= 0 \\ \lim_{n, t_2 \rightarrow \infty} |g_1^{\nu_\alpha}(\theta_0, \theta_1) - g_1(\theta_0, \theta_1)| &= 0 \end{cases}$$

$$\text{For any integer } n \in \mathbb{N}, \text{ if } t_2 = \lambda + n, \text{ then: } \lim_{\lambda, t_2 \rightarrow \infty} |g_0^{\nu_\alpha} - g_0| = 0.$$

A major implication of Lemma 2 is that with enough observations, $g_0^{\nu_\alpha}$ and $g_1^{\nu_\alpha}$ will eventually converge to the functions g_0 and g_1 . In fact, g_0^t approaches g_0 up to ν_α and then start degrading (as it ends up converging to g_1) whereas g_1^t becomes a better and better approximation of g_1 around ν_α and

improves asymptotically. As such, we are going to consider the following problem as proxy to the original QCD problem under unknown parameters (Equation (6)).

$$\hat{\nu}_\alpha = \underset{t}{\operatorname{argmin}} \{t | S_t^{\theta_0^t, \theta_1^t} > B_\alpha\} \quad \text{where} \quad \begin{cases} \theta_0^t = \underset{\theta}{\operatorname{argmin}} g_0^t(\theta, \theta_1^{t-1}) \\ \theta_1^t = \underset{\theta}{\operatorname{argmax}} g_1^t(\theta_0^{t-1}, \theta) \end{cases} . \quad (9)$$

The rational behind this choice is that around the change point, $S_t^{\theta_0^t, \theta_1^t}$ converges to $S_t^{\theta_0^*, \theta_1^*}$. Having access to a perfect evaluation of the functions g_0 and g_1 guarantees the fastest possible detection. In fact, ν_α – the optimal stopping time under known parameters – is a lower bound to the detection delay in the unknown parameter setting. In practice, only the first t observation are accessible to evaluate g_0^t and g_1^t . This introduces approximation errors to the estimates θ_0^t and θ_1^t , thus delaying the detection. However, this is not detrimental to the evaluation of the stopping time. Indeed:

Before ν_α : θ_0^t is a good estimator of θ_0^* and θ_1^t is a bad estimator of θ_1^* . In fact, the fraction of pre-change observations used to learn θ_1^* is of the order of $\min(1, \lambda/t)$. This helps maintaining a low log-likelihood ratio (equivalently maintain $S_t^{\theta_0^t, \theta_1^t}$ below the cutting threshold), as the estimation of θ_1^* will converge to a parameter close to θ_0^* .

After ν_α : θ_1^t is a good approximation of θ_1^* , but θ_0^t is a noisy estimation of θ_0^* (as post-change observations are used to learn it). The fraction of the data generated using θ_1^* but used to learn θ_0^* is proportional to $\frac{t-\nu_\alpha}{t}$. This favours – up to a certain horizon – higher log-likelihood ratio estimates (equivalently an incremental behaviour of the sequence $S_t^{\theta_0^t, \theta_1^t}$).

Distribution Approximation: In order to exploit the previously introduced results, a good approximation of $\mathbb{P}(\lambda | \nu_\alpha = n)$ is needed. If the observation satisfy Hypothesis 1, then the moments of $\mathbb{P}(\lambda | \nu_\alpha = n)$ up to the r^{th} order satisfy Equation (5).

When $r = \infty$, this is equivalent to the Hausdorff moment problem, which admits a unique solution that can be approximated with the generalised method of moments. In the remaining, we will however restrict ourselves to the case where $r = 2$, for tractability reasons even if there is an infinite number of distributions that satisfy Equation (5). However, there exists a unique solution to this problem if the underlying distribution belongs to some parametric family with exactly two parameters. Furthermore, uni-modal distributions (possibly centred around λ) are convenient for practical reasons. As a consequence, typical candidates are Binomial, Logistic, Normal, Beta and Weibull parametric families. Since computing the cumulative distribution functions is also necessary to evaluate the functions g_k^n , we will therefore focus on the Logistic distribution (whose cdf is a simple sigmoid function) as the appropriate parametric family to alleviate computational requirements.

For this reason, given θ_0, θ_1 , we approximate $\mathbb{P}(\lambda | \nu_\alpha = n)$ with $f_n^{\theta_0, \theta_1} = \text{Logistic}(\mu, s)$ where:

$$\mu = n - \frac{|\log(\alpha)|}{D_{KL}(f_{\theta_0} | f_{\theta_1}) + d} ; \quad s = \sqrt{3} \frac{|\log(\alpha)|}{\pi(D_{KL}(f_{\theta_0} | f_{\theta_1}) + d)} .$$

Verifying that $f_n^{\theta_0, \theta_1}$ satisfies Equation (5) for $m \leq 2$ is straightforward. As a consequence, $\mathbb{P}(\tau > t | \tau \sim f_n^{\theta_0, \theta_1})$ is a good approximation of $\mathbb{P}(\lambda > t | \nu_\alpha = n)$.

3.3 Limitations & practical solutions:

Solving the problem given by Equation (9) unfortunately yields poor performances for extreme values of the error threshold α . This is due to a degraded log-likelihood estimation both before λ and with $t \rightarrow \infty$. In fact, the log-likelihood ratios $L_t(X_{t+1} | X_t) := \log \frac{f_{\theta_1^t}}{f_{\theta_0^t}}(X_{t+1} | X_t)$ and the optimal log-likelihood ratios $L_t^*(X_{t+1} | X_t) = \log \frac{f_{\theta_1^*}}{f_{\theta_0^*}}(X_{t+1} | X_t)$ satisfy the following lemma:

Lemma 3 *The log-likelihood ratio L_t and L_t^* admit the following asymptotic behaviours:*

$$\lim_{\lambda \rightarrow \infty} \mathbb{E}_\lambda[L_\lambda^*] < 0 \text{ but } L_\lambda \xrightarrow[\lambda \rightarrow +\infty]{a.s.} 0 ; \quad \lim_{t \rightarrow \infty} \mathbb{E}_\lambda[L_t^* | \lambda < \infty] > 0 \text{ but } L_t \xrightarrow[t \rightarrow +\infty]{a.s.} 0 \quad (10)$$

Practically, this means that before the change point, the log likelihood ratio is over-estimated (as it should be smaller than 0), while after the change point, the log likelihood ratio is eventually

under-estimated (as it should exceed 0). This is a consequence of Lemma 2. In fact, for $t \gg \lambda$ (respectively for $t \leq \lambda$), both functions g_0^t and g_1^t are approaching g_1 (respectively g_0). Thus in both cases θ_0^t and θ_1^t converge to the same value. However, combined with the behaviour of g_0^t and g_1^t around ν_α from Lemma 2, we can expect the Kullback–Leibler (KL) divergence $D_{KL}(f_{\theta_0^t} \| f_{\theta_1^t})$ to converge to 0 before and after the change point while peaking around the optimal stopping time. We exploit this observation to mitigate the problems highlighted with Lemma 3.

Annealing: The under-estimation of L_t^* after the change point is due to the use of post change observations (drawn from $f_{\theta_1^*}$) when estimating θ_0^* . In practice, this is particularly problematic when the error rate must be controlled under a low threshold α (equivalently a high cutting threshold B_α) or when the pre and post change distributions are very similar. When t approaches the optimal stopping time ($t \approx \nu_\alpha$), the minimising argument of g_0^t is converging to θ_0^* . As t grows, the approximation g_0^t is degraded, while g_1^t is becoming a better approximation, thus θ_1^t starts converging to θ_1^* . This leads to an increase in the KL divergence. Our proposition is to keep optimising the version of g_0^t that coincides with this increase (which in turn is $g_0^{\nu_\alpha}$: the best candidate to identify θ_0^*). For this reason, we introduce the two following fixes:

1. Shift the probability $\mathbb{P}(\lambda > \tau | \nu_\alpha^S = n)$ by replacing it with $\mathbb{P}(\lambda > \tau - \Delta | \nu_\alpha^S = n)$ (where Δ is the ‘delay’ of the detection with respect to the Shiryaev stopping time: $(n - \nu_\alpha^S)^+$);
2. Anneal the optimisation steps of θ_0^t as the KL divergence increases.

These tweaks correct the objective function used to learn θ_0^* and stop its optimisation when the observations start to deviate from the learned pre-change distribution. The delay can be formally introduced by replacing g_0^t with $g_0^{t-\Delta}$ in Equation (9). In practice, Δ is a delay heuristic that increases as the KL divergence increases. This reduces the noise when learning θ_0^* . The second idea is to use a probability $p_0 = 1 - \Delta\epsilon$ of executing a gradient step when learning the pre-change parameter. This anneals the optimisation of θ_0^* .

Penalisation: The over-estimation of L_t^* before the change point, is due to the exclusive use of pre change observation when estimating θ_1^* . This is particularly problematic for application where a high error threshold is tolerable (or equivalently a low cutting threshold for the used statistic). This is also an issue when the pre- and post-change distributions are very different. As a solution, we penalise the log-likelihood using the inverse KL divergence. Before the change point, both parameters converge to θ_0^* : this means that the KL divergence between the estimated distributions is around 0. Inversely, after the change point, if the optimisation of θ_0^t is annealed, the KL divergence between the estimated parameters must hover around $D_{KL}(f_{\theta_0^*} \| f_{\theta_1^*})$. Formally, penalising the log likelihood can be seen as using \hat{L}_t when computing the statistics S_n where $\hat{L}_t = \max(L_t - c/D_{KL}(f_{\theta_0^*} \| f_{\theta_1^*}), L_{\min})$ for some real $c > 0$ and some minimum likelihood value L_{\min} to avoid arbitrarily small estimates.

We provide in the appendix an ablation analysis to prove their effectiveness.

Algorithm: In practice, only the first t observations are available in order to evaluate the parameters (θ_0^*, θ_1^*) . Hence, we design a stochastic gradient descent (SGD) based algorithm to solve Equation (9). Consider the following loss functions, where I is a set of time indices:

$$\begin{aligned} \mathcal{L}_0^n(I, \theta_0, \theta_1) &= \sum_{t \in I} \mathbb{P}(\tau < t | \tau \sim f_n^{\theta_0, \theta_1}) \log\left(\frac{f_{\theta_1}}{f_{\theta_0}}\right)(X_{t+1} | X_t) \\ \mathcal{L}_1^n(I, \theta_0, \theta_1) &= \sum_{t \in I} \mathbb{P}(\tau > t | \tau \sim f_n^{\theta_0, \theta_1}) \log\left(\frac{f_{\theta_1}}{f_{\theta_0}}\right)(X_{t+1} | X_t) \end{aligned} \quad (11)$$

The quantity \mathcal{L}_k^t is an estimator of g_k^t using the observations $(X_t)_{t \in I}$. The rational previously discussed implies that by re-weighting random samples from the observations we can approximate the functions g_k using the family of functions g_k^t , which is in turn approximated here with \mathcal{L}_k^t .

A good approximation of θ_0^t and θ_1^t can be obtained with few SGD steps. These parameters are used to update the SHIRYAEV or the CUSUM statistic. The change point is declared once the threshold B_α is exceeded. The proposed procedure is described in Algorithm 1. In addition to the classical SGD hyper-parameters (number of epochs, gradient step size, momentum, ...), we propose to control the **penalisation** and the **annealing** procedure using the coefficients $c, \epsilon \geq 0$ respectively.

Algorithm 1 Temporal Weight Redistribution

```

1: Procedure: TWR( $\theta^0, \theta^1, (X_t)_{t=0}^{t_2}, N_e, B_\alpha, \epsilon, c$ )
2: Initialise  $S \leftarrow 0$ ;  $\theta_0, \theta_1 \leftarrow \theta^0, \theta^1$ ;  $\Delta \leftarrow 0$ ; and  $p_0 \leftarrow 1$ 
3: while  $S \leq B_\alpha$  do
4:   for  $e \in [1, N_e]$  do
5:     Randomly sample  $I$ : a set of indices from  $[0, t]$ 
6:     Minimise  $\mathcal{L}_0^{t-\Delta}$  w.r.t  $\theta_0$  (with probability  $p_0$ ) and minimise  $\mathcal{L}_1^t$  w.r.t  $\theta_1$  (with probability 1)
7:      $S \leftarrow \text{statistic update rule}(S, \frac{f_{\theta_1}}{f_{\theta_0}}(X_{t+1}|X_t) - \frac{c}{D_{KL}(f_{\theta_0}|f_{\theta_1})})$ 
8:     If  $D_{KL}(f_{\theta_0}|f_{\theta_1}) > \bar{D}$  then  $\Delta \leftarrow \Delta + 1$  and  $p_0 \leftarrow p_0 - \epsilon$ 
9:      $\bar{D} \leftarrow \frac{t-1}{t}\bar{D} + \frac{1}{t}D_{KL}(f_{\theta_0}|f_{\theta_1})$ 

```

3.4 Theoretical guarantees for well-estimated likelihood ratio

The TWR algorithm updates an approximation of the SHIRYAEV or the CUSUM statistic S_n using the estimates \hat{L}_t . Under the assumption that there exist a set of constants $C_{\delta,t}$ such that $|\hat{L}_t - L_t^*| \leq C_{\delta,t}$ with probability $1 - \delta$, we derive the following performance bounds:

Lemma 4 *Given a finite set of observations $(X_t)_{t=0}^T$, let $\hat{\nu}_B$ (respectively ν_B^*) the stopping time using the estimates \hat{L}_t (respectively L_t^*) and the cutting threshold B . If $|\hat{L}_t - L_t^*| \leq C_{\delta,t}$ with probability $1 - \delta$, then there exist some positive constant κ such that with probability $1 - \delta$:*

$$ADD(\hat{\nu}_B) \leq ADD(\nu_{B+\kappa \sum_t C_{\delta,t}}^*); \quad PFA(\hat{\nu}_B) \leq PFA(\nu_{B-\kappa \sum_t C_{\delta,t}}^*) \quad (12)$$

The previous lemma guarantees with high probability that for well estimated likelihood ratios, the TWR detection has a better delay (respectively less false positives) than optimal approaches with a higher cutting threshold (respectively lower threshold). In addition, the performance gap is proportional to the cumulative errors $C_{\delta,t}$.

Notice, that after the change point λ , the estimates \hat{L}_t will converge to L_t^* as we get more observations (thus ensuring a decreasing behaviour of the errors $C_{\delta,t}$). However, before λ , it is impossible to guarantee a small error as only pre-change observations are available².

Nevertheless, we stress that the bounds provided by Lemma 4 are conservative. In practice, as long as $\hat{L}_t \leq L_t^* + C_\delta$ before the change point and $\hat{L}_t \geq L_t^* - C_\delta$ afterward (with probability $1 - \delta$ for some small constant C_δ), the evaluated statistic S_n will remain small before the change point and increase rapidly after it (as expected in the optimal detection algorithms). In the case of TWR, the annealing and penalisation procedures empirically guaranteed such behaviour.

4 Related works & complexity analysis

Previous work tackled QCD problem under unknown parameters for particular settings (i.i.d. observations drawn from an exponential family distributions) where they derive either Bayesian approaches to detect the change point [15] or provide asymptotic guarantees of detection for window-limited detection rules [16]. However these results do not generalise to more general settings, such as non i.i.d. observations without any constraints on the nature of the Markovian kernel f_θ .

In the general case, existing solutions for the QCD problem under known parameters have been extended to the case of unknown parameters using generalised likelihood ratio (GLR) statistics. For example, an optimal solution for the Lorden formulation is a generalisation of the CUSUM algorithm using the GLR statistic for testing the null hypothesis of no change-point, based on $(X_i)_0^n$, versus the alternative hypothesis of a single change-point prior to n . The GLR-based approaches enjoy strong convergence properties and achieve optimal performances in the unknown parameters setting [32, 21]. Without additional computation constraints, they provide an efficient solution to the QCD problems.

²We can however guarantee that the error $C_{delta, t < \lambda}$ is bounded (recall that $\hat{L}_t = \max(L_t - c/D_{KL}(f_{\theta_0^t} \| f_{\theta_1^t}), L_{min})$ and that before the change point $D_{KL}(f_{\theta_0^t} \| f_{\theta_1^t})$ is close to 0 as both θ_0^t and θ_1^t are estimated using pre-change observations.)

However, given n observation, GLR-based solution runs in $\mathcal{O}(n^2)$. Others approached the problem from a Bayesian perspective by keeping track of the run length posterior distribution (the time since the last change point). Since in practice this distribution is highly peaked, the Bayesian Online Change Point Detection (BOCPD) algorithm [1] is namely a good alternative in the i.i.d. setting. In fact, by pruning out run lengths with probabilities below ϵ or by considering only the K most probable run lengths, the algorithm runs respectively in $\mathcal{O}(n/\epsilon)$ and $\mathcal{O}(Kn)$ without critical loss of performance. Extensions of BOCPD algorithm to the case of non i.i.d observations, namely the Gaussian Process Change Point Models run in $\mathcal{O}(n^4)$ [29]. If pruning is applied, the complexity can be reduced to $\mathcal{O}(nR^2/\epsilon)$ where R is the typical unpruned length [29].

To avoid this complexity issue, multiple approximate solutions that run in $\mathcal{O}(1)$ have been proposed. However, a common practice [24, 17, 38, 33, 22] is to assume that pre-change parameters are known as this is not a major limitation in many applications (fault detection, quality control...) where the pre-change corresponds to nominal behaviour of a process and can be characterised offline. A sub-optimal solution [24] is to track in parallel $S_n^{\theta_0, \theta_1}$ over a subset of possible post-change distributions and consider the worst case scenario. Somewhat Similarly to our approach, adaptive algorithms [17, 33] attempt to improve this procedure by tracking $S_n^{\theta_0, \bar{\theta}_1}$ where $\bar{\theta}_1 = \operatorname{argmax}_{\theta} g_1(\theta_0, \theta)$. Orthogonally to the literature, our contribution is a procedure that exploits the asymptotic behaviour of Shirayev's optimal detection delay to approximate the posterior change point distribution. It can handle the case of unknown pre- and post- change parameters, runs in $\mathcal{O}(1)$, and have near optimal performances.

5 Experimental Results

The distribution family f_{θ} used experimentally to simulate data given the pre/post change parameters and the previous observations relies on two deep neural network $(\phi_{\mu}, \phi_{\sigma})$ used to evaluate the parameters of a Gaussian distribution such as: $f_{\theta}(\cdot|x) = \mathcal{N}(\phi_{\mu}(\theta, x), \phi_{\sigma}(\theta, x))$. It is possible to cover a wide range of parametric probability distribution families $\{f_{\theta}, \theta \in \Theta\}$ by sampling the neural networks parameters randomly $(\phi_{\mu}$ and $\phi_{\sigma})$ at each simulation. Averaging performances across these families assesses our algorithms great practical performances in multiple settings. Our algorithm is compared to three other possibilities: the optimal log-likelihood ratio (an oracle having access to the true parameters), the generalised log-likelihood ratio (GLR) and the adaptive log-likelihood ratio where the pre-change parameters are learned offline (a fraction of pre-change observations are used to learn θ_0). In this section, we quantify empirically the properties of the estimated Log-likelihood ratio using either the TWR algorithm or the adaptive one, as well as the detection delay (**ADD**) and the false alarm rate (**FAR**) gap between the constant complexity procedures and optimal ones.

We also introduce an alternative metric to the average detection delay: the regretted detection delay. An oracle with access to the true parameters will predict change as fast as the optimal algorithm under known parameters. In order to put performances into perspective, for a given cutting threshold B , the regretted average detection delay $\mathcal{R}_B(a)$ of an algorithm, is the additional delay with respect to the oracle. If we denote the oracle's optimal stopping time ν_B and the algorithm stopping time ν_B^a , then: $\mathcal{R}_B(a) = \mathbb{E}_{\lambda}[(\nu_B^a - \nu_B)^+ | \nu_B^a \geq \nu_B \geq \lambda]$. This formulation of the regret is conditioned to $\nu_B^a \geq \nu_B$ for the same reason that the measurement of the average detection delay is conditioned to $\nu_B \geq \lambda$. An algorithm that predicts change faster than the optimal one under known parameters, is over-fitting the noise in the data to some extent. For this reason, when comparing performances, there is no true added value in detecting changes faster than the optimal algorithm in the known parameter setting.

We evaluate the performances in the case where $\mathcal{X} = \mathbb{R}^{10}$, $\Theta = \mathbb{R}^{10}$, and $(\phi_{\mu}, \phi_{\sigma})$ are 5-layer deep, 32-neurons wide neural networks. In addition to sampling the neural networks parameters randomly at each run, we sample the parameters θ_0^* and θ_1^* such that the KL divergence between pre- and post- change distributions is $D_{KL}(f_{\theta_0^*} | f_{\theta_1^*}) = .3$. This allows us to view performances in difficult settings. For higher KL divergence values, change detection becomes easier. We provide in the appendix the same analysis for the case where $D_{KL}(f_{\theta_0^*} | f_{\theta_1^*}) = 3$. The reported performances are averaged over 500 simulations. In each one, the trajectory is 1000 sample long with a change point at the 500th observation. We use a pe-

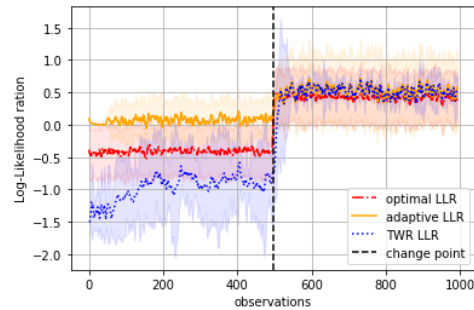


Figure 1: Estimated Log-likelihood ratio

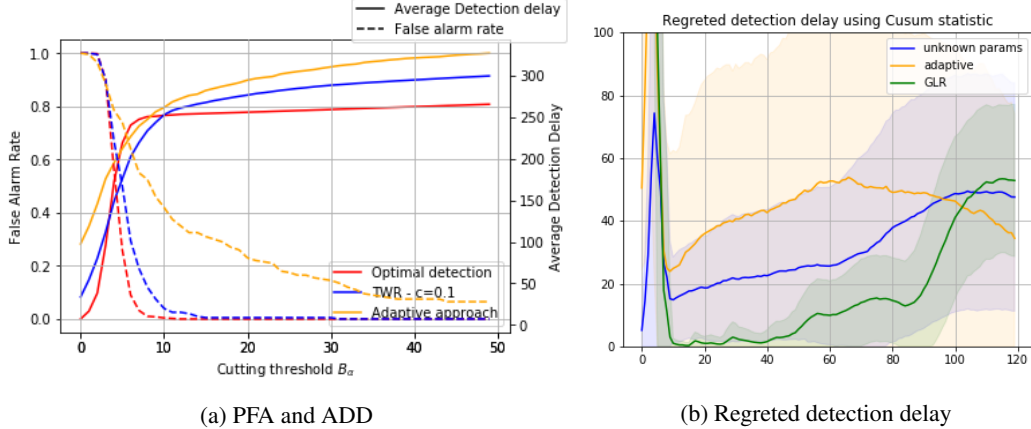


Figure 2: Performances of the CuSum updates as a function of B_α

nalisation coefficient $c = 0.1$, an annealing parameter $\epsilon = 0.01$, and a minimal LLR $L_{\min} = -1.5$ for the TWR algorithm. We also enable the adaptive approach to exploit 10% of the pre-change observations as it requires historical data to learn the pre-change parameter.

The average Log-likelihood ratios obtained during the training are reported in Figure 1. The ground truth (i.e. the optimal LLR represented with the red line) jumps rapidly from a negative value before the change point to a positive one. The TWR estimate (in blue) showcases a similar behaviour. As expected, before the change point, the log-likelihood remains negative (avoiding potential false alarms) without fitting L_t^* (as the post-change parameter estimates are performed using pre-change observations). After the change point, it converges quickly to a positive value close to the optimal LLR. On the other hand, the adaptive approach (the orange line) provides a good estimate of the post-change LLR, but behaves poorly before that. This is explained by the absence of a penalisation mechanism such as the one proposed in the TWR algorithm.

This is further confirmed in Figure 2a. In fact the reported **FAR** clearly demonstrate the inability of adaptive approaches to control the risk of false alarms. On the other hand, the TWR algorithm achieves a near optimal behaviour in this sense (as the blue curve is close to the red one).

Regarding the detection delay, the reported **ADD** demonstrate a similar logarithmic asymptotic behaviour of both the adaptive and the TWR approaches with a slight advantage for the latter. In addition, when analysing the regretted detection delay (Figure 2b), we notice that the TWR algorithm approaches the GLR performances (reported with the green line) asymptotically as we increased the cutting threshold B_α .

Overall, the TWR algorithm achieved comparable detection delays to those of the GLR based one (without requiring intensive computational resources) and controlled the false alarms risk in a near optimal fashion. We highlight that the alternative constant complexity algorithm (i.e. the adaptive approach) demonstrated a high degree of optimism with this regard as it provided a weak control of the false alarm rate. For the sake of completeness, we also provide in Appendix E additional experiments to demonstrate the ability of TWR to detect changes sequentially in multi-task settings.

6 Conclusion

We studied the QCD problem under unknown parameters for Markovian process. Extending our techniques to handle higher order Markov chains, (i.e., for some window parameter $w > 0$, f_θ depends of $X_{t-w:t}$ rather than just the last observation) is trivial, thus covering a wide range of natural processes. We provide a tractable algorithm with near optimal performances that relies on the asymptotic behaviour of optimal algorithms in the known parameter case. This mitigates the performance-cost dilemma providing the best of both worlds: a scalable procedure with low detection delay. Empirically, we were able to outperform previous approximate procedure (adaptive algorithms) and approach the performances of prohibitively expensive ones (GLR). Interesting future direction include taking into account the delay caused by the generalisation error.

References

- [1] R. P. Adams and D. J. C. MacKay. Bayesian online changepoint detection, 2007.
- [2] M. Andrychowicz, F. Wolski, A. Ray, J. Schneider, R. Fong, P. Welinder, B. McGrew, J. Tobin, O. Pieter Abbeel, and W. Zaremba. Hindsight experience replay. In I. Guyon, U. V. Luxburg, S. Bengio, H. Wallach, R. Fergus, S. Vishwanathan, and R. Garnett, editors, *Advances in Neural Information Processing Systems 30*, pages 5048–5058. Curran Associates, Inc., 2017.
- [3] M. Basseville, I. V. Nikiforov, et al. *Detection of abrupt changes: theory and application*, volume 104. prentice Hall Englewood Cliffs, 1993.
- [4] F. Caron, A. Doucet, and R. Gottardo. On-line changepoint detection and parameter estimation with application to genomic data. *Statistics and Computing*, 22(2):579–595, 2012.
- [5] D. C. Carslaw, K. Ropkins, and M. C. Bell. Change-point detection of gaseous and particulate traffic-related pollutants at a roadside location. *Environmental science & technology*, 40(22):6912–6918, 2006.
- [6] V. Draglia, A. G. Tartakovsky, and V. V. Veeravalli. Multihypothesis sequential probability ratio tests. i. asymptotic optimality. *IEEE Transactions on Information Theory*, 45(7):2448–2461, 1999.
- [7] A. Gleave and O. Habryka. Multi-task maximum entropy inverse reinforcement learning, 2018.
- [8] A. Gupta, R. Mendonca, Y. Liu, P. Abbeel, and S. Levine. Meta-reinforcement learning of structured exploration strategies. In *Advances in Neural Information Processing Systems*, pages 5302–5311, 2018.
- [9] T. Haarnoja, A. Zhou, P. Abbeel, and S. Levine. Soft actor-critic: Off-policy maximum entropy deep reinforcement learning with a stochastic actor, 2018.
- [10] M. Hairer. Convergence of markov processes. *Lecture notes*, 2010.
- [11] J. Ho and S. Ermon. Generative adversarial imitation learning, 2016.
- [12] T. L. Lai. On r-quick convergence and a conjecture of strassen. *The Annals of Probability*, pages 612–627, 1976.
- [13] T. L. Lai. Asymptotic optimality of invariant sequential probability ratio tests. *The Annals of Statistics*, pages 318–333, 1981.
- [14] T. L. Lai. Information bounds and quick detection of parameter changes in stochastic systems. *IEEE Transactions on Information Theory*, 44(7):2917–2929, 1998.
- [15] T. L. Lai, T. Liu, and H. Xing. A bayesian approach to sequential surveillance in exponential families. *Communications in Statistics—Theory and Methods*, 38(16-17):2958–2968, 2009.
- [16] T. L. Lai and H. Xing. Sequential change-point detection when the pre-and post-change parameters are unknown. *Sequential analysis*, 29(2):162–175, 2010.
- [17] C. Li, H. Dai, and H. Li. Adaptive quickest change detection with unknown parameter. In *2009 IEEE International Conference on Acoustics, Speech and Signal Processing*, pages 3241–3244. IEEE, 2009.
- [18] G. Lorden et al. Procedures for reacting to a change in distribution. *The Annals of Mathematical Statistics*, 42(6):1897–1908, 1971.
- [19] G. Lu, Y. Zhou, C. Lu, and X. Li. A novel framework of change-point detection for machine monitoring. *Mechanical Systems and Signal Processing*, 83:533–548, 2017.
- [20] L. Martí, N. Sanchez-Pi, J. M. Molina, and A. C. B. Garcia. Anomaly detection based on sensor data in petroleum industry applications. *Sensors*, 15(2):2774–2797, 2015.
- [21] Y. Mei et al. Sequential change-point detection when unknown parameters are present in the pre-change distribution. *The Annals of Statistics*, 34(1):92–122, 2006.

- [22] T. L. Molloy and J. J. Ford. Minimax robust quickest change detection in systems and signals with unknown transients. *IEEE Transactions on Automatic Control*, 64(7):2976–2982, 2018.
- [23] G. V. Moustakides et al. Optimal stopping times for detecting changes in distributions. *The Annals of Statistics*, 14(4):1379–1387, 1986.
- [24] I. V. Nikiforov. A suboptimal quadratic change detection scheme. *IEEE Transactions on Information Theory*, 46(6):2095–2107, 2000.
- [25] M. Plappert, M. Andrychowicz, A. Ray, B. McGrew, B. Baker, G. Powell, J. Schneider, J. Tobin, M. Chociej, P. Welinder, V. Kumar, and W. Zaremba. Multi-goal reinforcement learning: Challenging robotics environments and request for research, 2018.
- [26] M. Pollak. Optimal detection of a change in distribution. *The Annals of Statistics*, pages 206–227, 1985.
- [27] Y. Ritov. Decision theoretic optimality of the cusum procedure. *The Annals of Statistics*, pages 1464–1469, 1990.
- [28] G. J. Ross. Sequential change detection in the presence of unknown parameters. *Statistics and Computing*, 24(6):1017–1030, 2014.
- [29] Y. Saatchi, R. Turner, and C. Rasmussen. Gaussian process change point models, 08 2010.
- [30] O. Salem, Y. Liu, A. Mehaoua, and R. Boutaba. Online anomaly detection in wireless body area networks for reliable healthcare monitoring. *IEEE journal of biomedical and health informatics*, 18(5):1541–1551, 2014.
- [31] A. N. Shiryaev. On optimum methods in quickest detection problems. *Theory of Probability & Its Applications*, 8(1):22–46, 1963.
- [32] D. Siegmund and E. Venkatraman. Using the generalized likelihood ratio statistic for sequential detection of a change-point. *The Annals of Statistics*, pages 255–271, 1995.
- [33] V. Singamasetty, N. Nair, S. Bhashyam, and A. P. Kannu. Change detection with unknown post-change parameter using kiefer-wolfowitz method. In *2017 IEEE International Conference on Acoustics, Speech and Signal Processing (ICASSP)*, pages 3919–3923. IEEE, 2017.
- [34] A. G. Tartakovsky. On asymptotic optimality in sequential changepoint detection: Non-iid case. *IEEE Transactions on Information Theory*, 63(6):3433–3450, 2017.
- [35] A. G. Tartakovsky, M. Pollak, and A. S. Polunchenko. Third-order asymptotic optimality of the generalized shiryaev–roberts changepoint detection procedures. *Theory of Probability & Its Applications*, 56(3):457–484, 2012.
- [36] A. G. Tartakovsky and V. V. Veeravalli. General asymptotic bayesian theory of quickest change detection. *Theory of Probability & Its Applications*, 49(3):458–497, 2005.
- [37] Y. Teh, V. Bapst, W. M. Czarnecki, J. Quan, J. Kirkpatrick, R. Hadsell, N. Heess, and R. Pascanu. Distal: Robust multitask reinforcement learning. In *Advances in Neural Information Processing Systems*, pages 4496–4506, 2017.
- [38] J. Unnikrishnan, V. V. Veeravalli, and S. P. Meyn. Minimax robust quickest change detection. *IEEE Transactions on Information Theory*, 57(3):1604–1614, 2011.
- [39] V. V. Veeravalli and T. Banerjee. Quickest change detection. In *Academic Press Library in Signal Processing*, volume 3, pages 209–255. Elsevier, 2014.
- [40] K. Wang, H. Lu, L. Shu, and J. J. Rodrigues. A context-aware system architecture for leak point detection in the large-scale petrochemical industry. *IEEE Communications Magazine*, 52(6):62–69, 2014.
- [41] L. Yu, T. Yu, C. Finn, and S. Ermon. Meta-inverse reinforcement learning with probabilistic context variables, 2019.

Checklist

1. For all authors...
 - (a) Do the main claims made in the abstract and introduction accurately reflect the paper's contributions and scope? [Yes]
 - (b) Did you describe the limitations of your work? [Yes]
 - (c) Did you discuss any potential negative societal impacts of your work? [N/A]
 - (d) Have you read the ethics review guidelines and ensured that your paper conforms to them? [Yes]
2. If you are including theoretical results...
 - (a) Did you state the full set of assumptions of all theoretical results? [Yes]
 - (b) Did you include complete proofs of all theoretical results? [Yes]
3. If you ran experiments...
 - (a) Did you include the code, data, and instructions needed to reproduce the main experimental results (either in the supplemental material or as a URL)? [Yes] a complete description of the implementation is provided in the Appendix
 - (b) Did you specify all the training details (e.g., data splits, hyperparameters, how they were chosen)? [Yes]
 - (c) Did you report error bars (e.g., with respect to the random seed after running experiments multiple times)? [Yes]
 - (d) Did you include the total amount of compute and the type of resources used (e.g., type of GPUs, internal cluster, or cloud provider)? [N/A]
4. If you are using existing assets (e.g., code, data, models) or curating/releasing new assets...
 - (a) If your work uses existing assets, did you cite the creators? [Yes]
 - (b) Did you mention the license of the assets? [N/A]
 - (c) Did you include any new assets either in the supplemental material or as a URL? [N/A]
 - (d) Did you discuss whether and how consent was obtained from people whose data you're using/curating? [N/A]
 - (e) Did you discuss whether the data you are using/curating contains personally identifiable information or offensive content? [N/A]
5. If you used crowdsourcing or conducted research with human subjects...
 - (a) Did you include the full text of instructions given to participants and screenshots, if applicable? [N/A]
 - (b) Did you describe any potential participant risks, with links to Institutional Review Board (IRB) approvals, if applicable? [N/A]
 - (c) Did you include the estimated hourly wage paid to participants and the total amount spent on participant compensation? [N/A]

A Solution for the QCD problem under known parameters

In this section, we assume that both the parameters θ_0 and θ_1 in Equation (1) are known. We present in the following the main optimality existing results.

Min-Max formulation: In the i.i.d. case (i.e. when $f_\theta(\cdot|x) = f_\theta(\cdot)$), the CUSUM algorithm [18] is an optimal solution [23, 27] for the Lorden formulation (3). However, even though strong optimality results hold, optimising **WADD** is pessimistic. With the delay criterion base on **CADD** (Pollak formulation), algorithms based on the SHIRYAEV-ROBERTS statistic are asymptotically within a constant of the best possible performance [26, 35].

In the non i.i.d. case, state of the art methods [14] are modified versions of the CUSUM algorithm that converge asymptotically to a lower bound of **CADD** (and thus a lower bound to **WADD**).

Bayesian formulation: The SHIRYAEV algorithm [31] is asymptotically optimal in the i.i.d. case. This result is extended to the non i.i.d. case under Hypothesis 1 [36].

A.1 Algorithms

In this section, we formally introduce the algorithms used to solve the change point problems under known parameters. A common trait of these algorithms is the computation of a statistic $S_n^{\theta_0, \theta_1}$ and the definition of a cutting threshold B_α . The stopping time ν_α is the first time the statistic exceeds the threshold. The value B_α is chosen such that **PFA** (respectively **FAR**) of the associated stopping time does not exceed the level α . In the case of the BAYESIAN formulation, the threshold is simplified into $B_\alpha = \frac{1-\alpha}{\alpha}$.

The SHIRYAEV Algorithm: The general formulation of the statistic $S_n^{\theta_0, \theta_1}$, is the likelihood-ratio of the test of $H_0 : \lambda \leq n$ versus $H_1 : \lambda > n$ given the observations $X_{t \leq n}$. In the general case, with a prior $\mathbb{P}(\lambda = k) = \pi_k$, this statistic writes as:

$$S_n^{\theta_0, \theta_1} := \frac{\sum_{k \leq n} \pi_k \prod_{t=1}^{k-1} f_{\theta_0}(X_{t+1}|X^t) \prod_{t=k}^{n+1} f_{\theta_1}(X_{t+1}|X^t)}{\sum_{k > n} \pi_k \prod_{t=1}^{n-1} f_{\theta_0}(X_{t+1}|X^t)} \quad (13)$$

In the case of geometric prior with parameter ρ , the statistic is simplified into:

$$S_n^{\theta_0, \theta_1} = \frac{1}{(1-\rho)^n} \sum_{k=1}^n (1-\rho)^{k-1} \prod_{t=k}^n R_t(\theta_0, \theta_1) \text{ where } R_t(\theta_0, \theta_1) = \frac{f_{\theta_1}(X_{t+1}|X^t)}{f_{\theta_0}(X_{t+1}|X^t)}$$

The statistic $S_n^{\theta_0, \theta_1}$ can be computed recursively under this simplification:

$$S_0^{\theta_0, \theta_1} = 0 \text{ and } S_{n+1}^{\theta_0, \theta_1} = \frac{1+S_n^{\theta_0, \theta_1}}{1-\rho} R_{n+1}(\theta_0, \theta_1)$$

The SHIRYAEV-ROBERT Algorithm: The statistic to be computed in this case can be seen as an extension of the one in the SHIRYAEV algorithm when $\rho = 0$. The recursive formulation is indeed:

$$S_0^{\theta_0, \theta_1} = 0 \text{ and } S_{n+1}^{\theta_0, \theta_1} = (1 + S_n^{\theta_0, \theta_1}) R_{n+1}(\theta_0, \theta_1)$$

The CUSUM Algorithm: The relevant statistic is defined as:

$$S_n^{\theta_0, \theta_1} = \max_{k \leq n} \sum_{t=k}^n \log(R_t) \quad (14)$$

and can be computed recursively by:

$$S_0^{\theta_0, \theta_1} = 0 \text{ and } S_{n+1}^{\theta_0, \theta_1} = (S_n^{\theta_0, \theta_1} + \log(R_{n+1}))^+$$

B r-quick convergence hypothesis

We start by reminding the definition [34] of r -quick convergence:

Definition 1 Let $r > 0$, and $k, n \in \mathbb{N}$, we say that the normalised likelihood ratio $L_{k,n}$ converges r -quickly to a constant q as $n \rightarrow +\infty$ under probability \mathbb{P}^μ :

$$L_{k,n} = \frac{1}{n} \sum_{t=k}^{k+n} \frac{f_{\theta_1}(X_{t+1}|X_t)}{f_{\theta_0}(X_{t+1}|X_t)} \xrightarrow[n \rightarrow +\infty]{r\text{-quickly}} q \quad (15)$$

if $\mathbb{E}^\mu [L_{k,n}(\epsilon)]^T < \infty$ for any positive $\epsilon > 0$ where $L_{k,n}(\epsilon) = \sup\{n > 0 : \|L_{k,n} - q\| > \epsilon\}$ is the last time the normalised log-likelihood ratio leaves the interval $[q - \epsilon, q + \epsilon]$ [34].

Hypothesis 1 is not too restrictive, and r -quick convergence conditions were previously used to establish asymptotic optimality of sequential hypothesis tests for general statistical models [6, 12, 13].

Using the law of large numbers, this hypothesis is satisfied for $q = \mathbb{E}_{X_t \sim f_{\theta_1}} [\frac{f_{\theta_1}(X_t)}{f_{\theta_0}(X_t)}]$ in the i.i.d. case. In the (ergodic) Markovian case, the convergence is achieved for irreducible Markov chains due to their ergodicity.

However, the speed of convergence of Equation (4), depends on the speed of convergence to the stationary distribution of the Markov chain. Even though for any $r > 0$ construction of Markov chains that satisfy assumption 4 is possible [6], providing a guarantee of this speed is not a trivial question [10].

C Algorithmic analysis

C.1 Impact analysis (annealing and penalisation)

In order to justify experimentally the use of annealing and penalisation to solve the issues highlighted with Lemma 3, we simulate simple examples where the phenomena are amplified to their extreme.

Annealing: We consider a one dimensional signal. The KL divergence between the pre and post change distribution is 0.06. As discussed in the paper, the issue is that after the change point we start using observations from the post change distribution to learn the pre change one. This leads to θ_0^t and θ_1^t converging to the post change parameter θ_1^* . In fact, without the annealing procedure, the KL divergence $D_{\text{KL}}(f_{\theta_0^t} \| f_{\theta_1^*})$ (the blue curve, in the top right subplot in Figure 3) ends up collapsing to 0. This has the problematic consequence of slowing down the statistics. In fact, both the SHIRYAEV and the CUSUM statistics (the blue curves in the lower subplots of Figure 3) start adjacent to the optimal statistic (in red) and slowly degrade in quality. On the other hand, implementing the annealing procedure -as described in the paper with a step size $\epsilon = 0.01$ - solves this issue. The KL divergence (green curve) hovers around the true value and the computed statistics are almost within a constant of the optimal one.

Penalising: We consider in this case a one dimensional signal with a KL divergence of 2. The problem we are analysing in this setting is the exclusive use of pre change observations when learning the parameters before the change point. The optimal log-likelihood ratio (LLR) before the change point is -2 (the red curve in the top right subplot of Figure 4) while the learned one (in blue) is around 0. This is due to θ_0^t and θ_1^t converging to the pre change parameter θ_0^* . This over-estimation of the LLR leads to a higher estimate of the SHIRYAEV statistic. In the lower left subplot of Figure 4, we have an increase of 100 fold compared to the optimal value. Penalising the LLR, using a coefficient $c = 0.01$, solves this issue without being detrimental to the post change performance. In fact the penalised LLR (the green curve) is strictly negative before the change point and has a similar values to the optimal ones afterwards. The associated SHIRYAEV statistic (the green curve) is less prone to detect false positives as it has the same behaviour as the optimal one. This safety break (penalisation) comes with a slight drawback for higher cutting thresholds as it induces an additional delay due to the penalising component. Interestingly, the CUSUM statistic does not have the same behaviour in this example. This is explained with the nature of the LORDEN formulation. As it minimises a pessimistic evaluation of the delay (**WADD**), the impact of a LLR of 0 is less visible. However, on average, the same phenomena occurs. This will be observed in the ablation analysis, where on average, there was no notable differences between the different formulations.

C.2 Ablation analysis (annealing and penalisation)

Since the algorithm integrates different ideas to mitigate the issues discussed in the paper, an ablation study is conducted to understand their contribution. We simulate the case where $\mathcal{X} = \mathbb{R}^{10}$, $\Theta = \mathbb{R}^{10}$,

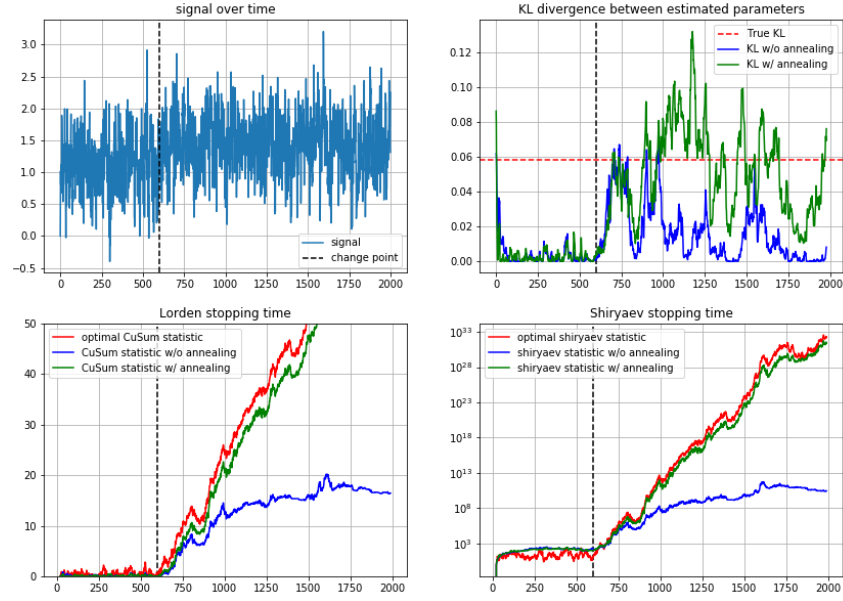


Figure 3: Annealing the optimisation of θ_0

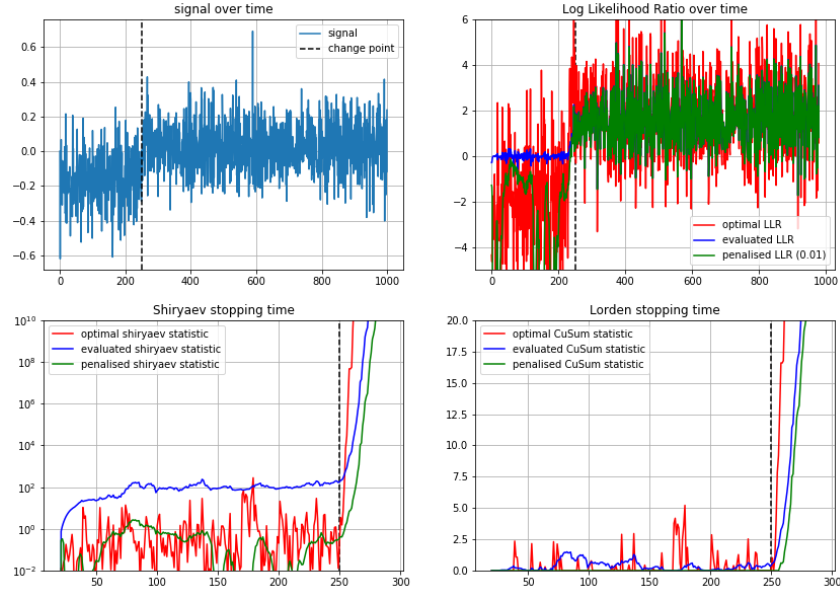


Figure 4: Penalising the Log Likelihood Ratio

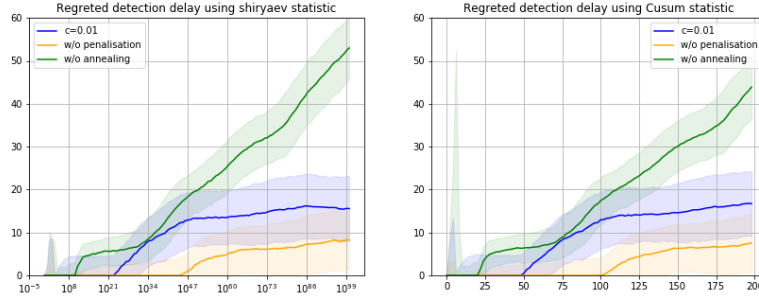
and (ϕ_μ, ϕ_σ) are 5-layer deep, 32-neurons wide neural network. The penalisation coefficient is fixed to 0.01 and the annealing step is fixed to 0.02. In Figure 5, the regretted detection delay is evaluated using 500 simulations. We consider a mid-ground complexity case, with a KL divergence of 1.5, which is a more realistic scenario in real life situations.

We provide the regret with respect to both the optimal performance under known parameters for both the BAYESIAN setting (SHIRYAEV statistic on the left) and the MIN-MAX setting (CUSUM statistic on the right). We split the analysis of the curves to three scenarios: The low, the mid and the high cutting threshold cases. They correspond respectively to 3 categories of risk inclinations levels: the high, the mid and the low.

The high risk inclination: In the presented case, this correspond to a cutting threshold B smaller than 10^{20} in the shiryaev algorithm and than 50 in the CUSUM algorithm. This can be associated to household applications and relatively simple settings with high reaction time. In this case, the simplest version of the algorithm is sufficient to achieve relatively small regret values. In fact, the green curve (associated to the configuration without annealing) presents a relatively low regret with respect to the optimal delay.

The low risk inclination: In the presented case, this correspond to B higher than 10^{50} in the shiryaev algorithm and than 100 in the cusum algorithm. This can be associated to critical applications where precision outweighs the benefice of speed such as energy production. In this case, configurations without annealing (presented in green here) have poor performance. The best configuration is to perform annealing but without penalisation of the log likelihood.

The intermediate risk inclination: This coincides with the remaining spectrum of cases. For example, when the application is critical but requires high reaction time, or when the application has no reaction time constraints but doesn't require extreme safety measures. In this setting, we observe that the best performance require some amount of penalisation of the log likelihood. The choice of the coefficient should be guided by the KL divergence between the pre and post change distributions, with $c = 0$ when the change is subtle (small KL).



(a) $D_{KL}(f_{\theta_0^*} | f_{\theta_1^*}) = 1.5$

Figure 5: Ablation analysis of the regret detection delay as a function of the cutting threshold

C.3 Divergence measures based algorithmic variant

In order to solve the QCD problem under unknown parameters, we propose in this paper to approximate the log-likelihood ratio L_t^* efficiently. We achieved this by optimising a surrogate of the KL divergence between the estimated parameters (θ_t^0, θ_t^1) and the true parameters (θ_0^*, θ_1^*) . Algorithm 1 devises a theoretically grounded weighting technique that approximates expectations under pre/post change distributions. For this reason, other divergence measure based loss functions can be used instead of the proposed ones in Equation 11. In particular, consider the following loss functions:

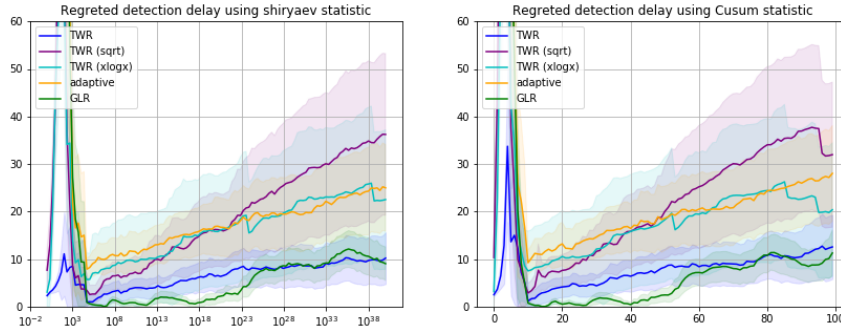
$$\begin{aligned}\mathcal{L}_0^n(I, \theta_0, \theta_1, g) &= \sum_{t \in I} \mathbb{P}(\tau < t | \tau \sim f_n^{\theta_0, \theta_1}) g\left(\frac{f_{\theta_1}}{f_{\theta_0}}\right)(X_{t+1} | X_t) \\ \mathcal{L}_1^n(I, \theta_0, \theta_1, g) &= \sum_{t \in I} \mathbb{P}(\tau > t | \tau \sim f_n^{\theta_0, \theta_1}) g\left(\frac{f_{\theta_1}}{f_{\theta_0}}\right)(X_{t+1} | X_t)\end{aligned}$$

For $k \in \{0, 1\}$, the loss function $\mathcal{L}_k^n(I, \theta_0, \theta_1, g)$ approximates $\mathbb{E}_k[g(\frac{f_{\theta_1}}{f_{\theta_0}})]$. Under the assumptions that g is an increasing function with $g(1) = 0$ and $h(x) = x.g(x)$ is convex, \mathcal{L}_0^n becomes a proxy

of the h -divergence measure $D_h(f_{\theta_1^*} \| f_{\theta_0^*})$ (respectively $D_h(f_{\theta_0^*} \| f_{\theta_1^*})$ for \mathcal{L}_1^n). This formulation is coherent with the QCD objective as it minimises L_t under the pre-change distribution and maximises it under the post change distribution and we can use it as a valid change point detection algorithm. The obtained parameters (θ_t^0, θ_t^1) are the furthest apart with respect to the associated h -divergence. The KL divergence (associated with $g(x) = \log(x)$) is a natural fit for our setting as it simultaneously ensures that the evaluated parameters converge to (θ_0^*, θ_1^*) .

We keep using the same hyper-parameters from the ablation analysis in order to asses the **ADD** of the TWR algorithm using different divergence measures. The experimental results are reported in Figure 6. In addition to the KL-based version (dark blue curve), we consider the case where $g(x) = \sqrt{x} - 1$ (purple curve) and the case where $g(x) = (x - 1) \cdot \log(x)$ (cyan curve). We also provide the adaptive (yellow) and GLR (green) average detection delay as a baseline.

The KL-divergence based approach provides comparable **ADD** to the GLR, outperforming both the adaptive algorithm and the other variant of the TWR.



(a) $D_{KL}(f_{\theta_0^*} \| f_{\theta_1^*}) = 1.5$

Figure 6: Regretted average detection delay using different divergence measures

D Proofs of technical results

Proof of Lemma 1: We start by observing the following:

$$\begin{cases} g_0(\theta, \theta_1) = \mathbb{E}_0 \left[\log \left(\frac{f_{\theta_1}}{f_{\theta_0^*}} \right) \right] + \mathbb{E}_0 \left[\log \left(\frac{f_{\theta_0^*}}{f_{\theta}} \right) \right] \\ g_1(\theta_0, \theta) = \mathbb{E}_1 \left[\log \left(\frac{f_{\theta_1^*}}{f_{\theta_0}} \right) \right] - \mathbb{E}_1 \left[\log \left(\frac{f_{\theta_1^*}}{f_{\theta}} \right) \right] \end{cases}$$

Notice that both quantities $\mathbb{E}_0 \left[\log \left(\frac{f_{\theta_1}}{f_{\theta_0^*}} \right) \right]$ and $\mathbb{E}_1 \left[\log \left(\frac{f_{\theta_1^*}}{f_{\theta_0}} \right) \right]$ are constants with respect to the parameter θ , and that:

$$\begin{cases} \mathbb{E}_0 \left[\log \left(\frac{f_{\theta_0^*}}{f_{\theta}} \right) \right] = D_{KL}(f_{\theta_0^*} \| f_{\theta}) \\ \mathbb{E}_1 \left[\log \left(\frac{f_{\theta_1^*}}{f_{\theta}} \right) \right] = D_{KL}(f_{\theta_1^*} \| f_{\theta}) \end{cases}$$

where D_{KL} is the Kullback–Leibler divergence in the i.i.d case and the Kullback–Leibler divergence rate in the Markov chains case, i.e.

$$D_{KL}(f_{\theta_0} \| f_{\theta_1}) = \begin{cases} \int_x f_{\theta_0}(x) \log \left(\frac{f_{\theta_0}}{f_{\theta_1}} \right)(x) \\ \int_x \Pi_0(x) \int_y f_{\theta_0}(y|x) \log \left(\frac{f_{\theta_0}}{f_{\theta_1}} \right)(y|x) \end{cases}$$

When well defined, $D_{KL}(f_{\theta_0} \| f_{\theta_1})$ is strictly positive except when $f_{\theta_0} = f_{\theta_1}$. This allows us to conclude that:

$$\begin{cases} \operatorname{argmin}_{\theta} g_0(\theta, \theta_1) = \operatorname{argmin}_{\theta} D_{KL}(f_{\theta_0^*} \| f_{\theta}) = \theta_0^* \\ \operatorname{argmax}_{\theta} g_1(\theta_0, \theta) = \operatorname{argmax}_{\theta} -D_{KL}(f_{\theta_1^*} \| f_{\theta}) = \theta_1^* \end{cases}$$

This concludes the proof of the Lemma.

Proof of Lemma 2: We denote μ_0 the initial distribution according to which X_0 is sampled and μ_t the distribution of X_t . We re-write the functions g_k^n as:

$$\begin{aligned} g_0^n(\theta_0, \theta_1) &= \sum_{t=0}^{t_2} \frac{\mathbb{P}(\lambda > t | \nu_\alpha = n)}{\sum_{i=0}^{t_2} \mathbb{P}(\lambda > i | \nu_\alpha = n)} \mathbb{E}_{0,t}[\log(\frac{f_{\theta_1}}{f_{\theta_0}})(X|X_p)] \\ g_1^n(\theta_0, \theta_1) &= \sum_{t=0}^{t_2} \frac{\mathbb{P}(\lambda < t | \nu_\alpha = n)}{\sum_{i=0}^{t_2} \mathbb{P}(\lambda < i | \nu_\alpha = n)} \mathbb{E}_{1,t}[\log(\frac{f_{\theta_1}}{f_{\theta_0}})(X|X_p)] \end{aligned}$$

where $\mathbb{E}_{k,t}$ is taken with respect to $(X_p, X) \sim \mu_t(X_p) \times (f_{\theta_0}^*(X|X_p)\mathbb{1}_{t < \lambda} + f_{\theta_1}^*(X|X_p)\mathbb{1}_{t > \lambda})$. It's important to notice for what follows that $\mathbb{P}(\lambda > t | \nu_\alpha = n)$ is non-decreasing with respect to t . We also highlight that for any finite set I , we have the following:

$$\sum_{t \in I} \frac{\mathbb{P}(\lambda < t | \nu_\alpha = n)}{\sum_{i=0}^{t_2} \mathbb{P}(\lambda < i | \nu_\alpha = n)} \xrightarrow{n, t_2 \rightarrow \infty} 0$$

On the other hand, $\mathbb{P}(\lambda > t | \nu_\alpha = n)$ is non-increasing with respect to t . This implies that there exist some constant h_α such that: $\mathbb{P}(\lambda > i | i < \nu_\alpha = n) > \mathbb{P}(\lambda > \nu_\alpha) > h_\alpha > 0$ (where the second part of the inequality is guaranteed by construction [36]). As $n \rightarrow \infty$, it follows that:

$$\sum_{t \in I} \frac{\mathbb{P}(\lambda > t | \nu_\alpha = n)}{\sum_{i=0}^{t_2} \mathbb{P}(\lambda > i | \nu_\alpha = n)} \xrightarrow{n, t_2 \rightarrow \infty} 0$$

Consider the case where $\lambda = \infty$. As X_t is a irreducible Markov chain, we have that

$$\|\Pi_0^* - \mu_t\|_{\text{T.V}} \xrightarrow{t \rightarrow \infty} 0$$

where $\|\cdot\|_{\text{T.V}}$ is the total variation norm. This means that for any small value $\epsilon > 0$, there exist $T > 0$ such that:

$$\forall t \geq T \quad \|\Pi_0^* - \mu_t\|_{\text{T.V}} \leq \epsilon$$

Thus, as the observation X_t are bounded, we have for any continuous function f , there exist $T_\epsilon > 0$ such that:

$$\forall t \geq T_\epsilon \quad |\mathbb{E}_{k,t}[f(X|X_p)] - \mathbb{E}_0[f(X|X_p)]| \leq \epsilon$$

This implies that when $\lambda = \infty$ then g_0^∞ and g_1^∞ converges to g_0 . In fact for any ϵ , there exist N and T_2 such that for all $n > N$:

$$\begin{aligned} \forall t_2 \geq T_2 \quad \sum_{t < T_\epsilon} \frac{\mathbb{P}(\lambda < t | \nu_\alpha = n)}{\sum_{i=0}^{t_2} \mathbb{P}(\lambda < i | \nu_\alpha = n)} &\leq \epsilon \\ \forall t_2 \geq T_2 \quad \sum_{t < T_\epsilon} \frac{\mathbb{P}(\lambda > t | \nu_\alpha = n)}{\sum_{i=0}^{t_2} \mathbb{P}(\lambda > i | \nu_\alpha = n)} &\leq \epsilon \\ \forall t_2 \geq t \geq T_\epsilon \quad |\mathbb{E}_{k,t}[f(X|X_p)] - \mathbb{E}_0[f(X|X_p)]| &\leq \epsilon \end{aligned}$$

The case where λ is finite can be deduced by considering the sequence $X_{t > \lambda}$. All the observation are sampled according to $f_{\theta_1}^*$, and thus g_0^∞ and g_1^∞ converges to g_1 .

This result is also valid for $g_1^{\nu_\alpha}$. In fact, as $\mathbb{P}(t > \lambda | \nu_\alpha = n)$ is increasing with respect to t , then for any fixed horizon H we have:

$$\sum_{t < H} \frac{\mathbb{P}(\lambda < t | \nu_\alpha = n)}{\sum_{i=0}^{t_2} \mathbb{P}(\lambda < i | \nu_\alpha = n)} \xrightarrow{t_2 \rightarrow \infty} 0.$$

As this remains true for $H = T_\epsilon$, we obtain that $g_1^{\nu_\alpha}$ converges to g_1 .

For a given integer n , if $t_2 = \lambda + n$, the convergence of $g_0^{\nu_\alpha}$ to g_0 is achieved as $\lambda \rightarrow \infty$. In order to establish this result, we need to prove that $\sum_{t=\lambda}^{t_2} \frac{\mathbb{P}(t < \lambda | \nu_\alpha)}{\sum_{i=0}^{t_2} \mathbb{P}(i < \lambda | \nu_\alpha)}$ is decreasing with respect to λ .

This is a consequence of $\mathbb{P}(t < \lambda | \nu_\alpha)$ being decreasing with respect to t . In fact:

$$\begin{aligned} \sum_{t=\lambda}^{t_2} \mathbb{P}(\lambda > t | \nu_\alpha) &\leq \sum_{t=\lambda}^{t_2} \mathbb{P}(\lambda > \lambda | \nu_\alpha) = n \mathbb{P}(\lambda > \lambda | \nu_\alpha) \\ \sum_{t=0}^{t_2} \mathbb{P}(\lambda > t | \nu_\alpha) &\geq \sum_{t=0}^{\lambda} \mathbb{P}(\lambda > \lambda | \nu_\alpha) = \lambda \mathbb{P}(\lambda > \lambda | \nu_\alpha) \end{aligned}$$

as a consequence the following inequality holds:

$$\sum_{t=\lambda}^{t_2} \frac{\mathbb{P}(\lambda > t | \nu_\alpha)}{\sum_{i=0}^{t_2} \mathbb{P}(\lambda > i | \nu_\alpha)} \leq \frac{n}{\lambda} \xrightarrow{\lambda \rightarrow \infty} 0.$$

As such, for any $\epsilon > 0$, there exists $A_n > 0$ such that:

$$\begin{aligned} \forall \lambda \geq A_n \quad \sum_{t=\lambda}^{t_2} \frac{\mathbb{P}(\lambda > t | \nu_\alpha)}{\sum_{i=0}^{t_2} \mathbb{P}(\lambda > i | \nu_\alpha)} &\leq \epsilon \\ \forall \lambda \geq T_\epsilon \quad \sum_{t=0}^{T_\epsilon} \frac{\mathbb{P}(\lambda > t | \nu_\alpha)}{\sum_{i=0}^{t_2} \mathbb{P}(\lambda > i | \nu_\alpha)} &\leq \epsilon \\ \forall \lambda \geq t \geq T_\epsilon \quad |\mathbb{E}_{0,t}[f(X|X_p)] - \mathbb{E}_0[f(X|X_p)]| &\leq \epsilon \end{aligned}$$

Proof of Lemma 3: We have g_k^λ converges to g_0 as $\lambda \rightarrow \infty$ (respectively g_k^t converges to g_1 as $t \rightarrow \infty$). Given that θ_0^* minimises g_0 (respectively θ_1^* minimises g_1), then θ_k^λ and θ_k^t satisfy the following:

$$\theta_0^\lambda, \theta_1^\lambda \xrightarrow[\lambda \rightarrow +\infty]{\text{a.s.}} \theta_0^* \quad \text{and} \quad \theta_0^t, \theta_1^t \xrightarrow[t \rightarrow +\infty]{\text{a.s.}} \theta_1^*.$$

As such, we obtain the following result:

$$L_\lambda \xrightarrow[\lambda \rightarrow +\infty]{\text{a.s.}} 0 \quad \text{and} \quad L_t \xrightarrow[t \rightarrow +\infty]{\text{a.s.}} 0$$

On the other hand we have the following:

$$\begin{aligned} \lim_{\lambda \rightarrow \infty} \mathbb{E}_\lambda[L_\lambda^*] &= \mathbb{E}_{X_{\lambda-1} \sim \Pi_0^*, X_\lambda \sim f_{\theta_0^*}}[L_\lambda^*] = -D_{K.L}(f_{\theta_0^*} \| f_{\theta_1^*}) < 0 \\ \lim_{t \rightarrow \infty} \mathbb{E}_\lambda[L_t^*] &= \mathbb{E}_{X_{t-1} \sim \Pi_1^*, X_t \sim f_{\theta_1^*}}[L_t^*] = D_{K.L}(f_{\theta_0^*} \| f_{\theta_1^*}) > 0 \end{aligned}$$

This concludes the proof of the lemma.

Proof of Lemma 4: We prove the result of this lemma for both the SHIRYAEV and the CUSUM statistics. For this reason, we start by establishing that for any integer n , there exist some constant κ_n such that with probability $1 - \delta$:

$$|\hat{S}_n - S_n^*| \leq \kappa_n \sum_{t=0}^n C_{\delta,t} \tag{16}$$

1- The SHIRYAEV statistic: We prove this case using an induction over the indices n . Recall that:

$$S_{n+1} = \frac{1 + S_n}{1 - \rho} L_{n+1}, \text{ and } S_0 = 0$$

The base case is trivially verified. For the induction step, notice that with probability $1 - \delta$:

$$\begin{aligned} \left| \frac{1 + S_n^*}{1 - \rho} - \frac{1 + \hat{S}_n}{1 - \rho} \right| &\leq \frac{\kappa \sum_{t=0}^n C_{\delta,t}}{1 - \rho} \\ |L_{n+1}^* - \hat{L}_{n+1}| &\leq C_{\delta,n+1} \end{aligned}$$

Given that the likelihood ratio is bounded (i.e. there is $a, b > 0$ such that $L_t^*, \hat{L}_t \in [a, b]$ for any index t), and that the logarithmic function is $\frac{1}{a}$ -Lipschitz continuous on $[a, b]$, it follows that there exist some constant $K > 0$ such that with probability $1 - \delta$:

$$\begin{aligned} \left| \log\left(\frac{1 + S_n^*}{1 - \rho}\right) - \log\left(\frac{1 + \hat{S}_n}{1 - \rho}\right) \right| &\leq K \frac{\kappa \sum_{t=0}^n C_{\delta,t}}{1 - \rho} \\ |\log(L_{n+1}^*) - \log(\hat{L}_{n+1})| &\leq KC_{\delta,n+1} \end{aligned}$$

This implies that with probability $1 - \delta$:

$$|\log(\hat{S}_{n+1}) - \log(S_{n+1}^*)| \leq K \frac{\kappa \sum_{t=0}^n C_{\delta,t} + (1 - \rho)C_{\delta,n+1}}{1 - \rho} \leq K \frac{\kappa \sum_{t=0}^{n+1} C_{\delta,t}}{1 - \rho}$$

Similarly, the estimated statistics are also bounded (due to the boundedness of the likelihood ratio) which implies that there exist some constant K' such that with probability $1 - \delta$:

$$|\hat{S}_{n+1} - S_{n+1}^*| \leq \frac{KK'\kappa}{1 - \rho} \sum_{t=0}^{n+1} C_{\delta,t} \leq \kappa' \sum_{t=0}^{n+1} C_{\delta,t}$$

2- The CUSUM statistic: Recall that:

$$S_n = \max_{k \leq n} \sum_{t=k}^n \log(L_t)$$

As the log-likelihood ratio is bounded, and the logarithmic function is Lipschitz continuous on any interval $[a, b]$ where $a, b > 0$, it follows that there exist some constant K such that with probability $1 - \delta$:

$$|\log(L_n^*) - \log(\hat{L}_n)| \leq KC_{\delta,n}$$

For this reason, it follows that for any integer $k \leq n$, and with probability $1 - \delta$:

$$\left| \sum_{t=k}^n \log(L_t^*) - \sum_{t=k}^n \log(\hat{L}_t) \right| \leq K \sum_{t=k}^n C_{\delta,t}$$

Given that the constants $C_{\delta,t}$ are positive for any integer t , we get with probability $1 - \delta$:

$$|\hat{S}_n - S_n^*| \leq K \max_{k \leq n} \sum_{t=k}^n C_{\delta,t} \leq \kappa \sum_{t=0}^n C_{\delta,t}$$

Now that we proved Equation 16 for both the SHIRYAEV and the CUSUM statistics, we derive the bounds stated in Lemma 4. In the following, let $\kappa = \max_{k \leq T} \kappa_n$. For the sake of simplicity, we will bound the inequality conservatively using the worst case cumulative errors, i.e. for any integer $n \leq T$ we have:

$$|\hat{S}_n - S_n^*| \leq \kappa \sum_{t=0}^T C_{\delta,t} \quad (17)$$

A- Average Detection Delay: From Equation 17, we derive that:

$$\mathbb{P}(\min_t S_t^* - \kappa \sum_{k=0}^T C_{\delta,k} \leq \min_t \hat{S}_t \leq \min_t S_t^* + \kappa \sum_{k=0}^T C_{\delta,k}) = 1 - \delta$$

Which in turn implies that for any $t \leq T$:

$$\mathbb{P}(\min_t \hat{S}_t + \kappa \sum_{k=0}^T C_{\delta,k} \geq \min_t S_t^*) \geq 1 - \delta$$

For any given threshold B , it follows that with probability $1 - \delta$ the the optimal statistic exceeds B after that $\hat{S}_t + \kappa \sum_{k=0}^T C_{\delta,k}$ reached the same threshold. Equivalently this can be written as:

$$\mathbb{P}\left(\left[\arg\min_t \hat{S}_t \geq B - \kappa \sum_{k=0}^T C_{\delta,k}\right] \leq \left[\arg\min_t S_t^* \geq B\right]\right) \geq 1 - \delta$$

By averaging with respect to the true cutting threshold λ we obtain with probability at least $1 - \delta$:

$$\mathbf{ADD}(\hat{\nu}_B) \leq \mathbf{ADD}(\nu_{B+\kappa \sum_t C_{\delta,t}}^*)$$

B- Probability of False Alarms: Similarly, we derive from Equation 17 that:

$$\mathbb{P}(\min_t S_t^* - \kappa \sum_{k=0}^T C_{\delta,k} \leq \min_t \hat{S}_t \leq \min_t S_t^* + \kappa \sum_{k=0}^T C_{\delta,k}) = 1 - \delta$$

Which in turn implies that for any $t \leq T$:

$$\mathbb{P}(\max_t \hat{S}_t - \kappa \sum_{k=0}^T C_{\delta,k} \leq \max_t S_t^*) \geq 1 - \delta$$

In other words, for any given threshold B , with probability $1 - \delta$, if the optimal statistic S_t^* did not exceed B , nor would $\hat{S}_t - \kappa \sum_{k=0}^T C_{\delta,k}$. In particular, if there is no change point, we get with probability at least $1 - \delta$:

$$\mathbb{P}(\max_t \hat{S}_t \geq B + \kappa \sum_{k=0}^T C_{\delta,k}) \leq \mathbb{P}(\max_t S_t^* \geq B)$$

Or, equivalently:

$$\mathbf{PFA}(\hat{\nu}_B) \leq \mathbf{PFA}(\nu_{B-\kappa \sum_t C_{\delta,t}}^*)$$

E Additional experimental results

E.1 Hyper-parameter selection

The algorithm we designed requires the selection of a few hyper-parameters in order to run properly. In this section we address the issue of tuning them.

The first set of parameters are for optimisation purpose, and thus we advise selecting them according to the complexity of the probability distribution family $\{f_\theta, \theta \in \Theta\}$. In all the experimental settings we used a batch size of 32, a number of epoch equal to 25 and a gradient step size of 0.001. The initial task parameters θ^0 and θ^1 are chosen randomly unless stated otherwise.

As for the cutting threshold, the penalisation and the annealing coefficients, they depend on the KL divergence between the pre- and post- change distribution (thus the task sampling distribution \mathcal{F}) and on the mixing times of these distribution. Fine tuning using grid search is the most efficient way to identify suitable candidates.

From our experimental inquiries, we advise a low penalisation coefficient (e.g. $c = 0.001$) unless the threshold B_α is smaller than 100 for the SHIRYAEV statistic and smaller than 10 for the CUSUM statistic. The annealing parameter ϵ depends on the mixing time of the Markov chain. In fact ϵ reflects to what extent we keep learning the pre-change parameter once it's similar to the post-change one. In practice we found out that a small coefficient (e.g. $\epsilon = 0.01$) is advised when the observations converge slowly to the stationary distribution. On the other hand, when convergence occurs in few observations, a higher coefficient is a safer choice.

E.2 Copycat agent problem: sequentially detecting changes

Consider a task space Θ and for each task $\theta \in \Theta$ the associated Markov decision process $\mathcal{M}_\theta = \{\mathcal{S}, \mathcal{A}, \mathcal{P}, \mathcal{R}_\theta, \gamma\}$ where \mathcal{S} is the state space, \mathcal{A} is the action space, \mathcal{P} is the environment dynamics, \mathcal{R}_θ is the task specific reward function and γ is the discount factor. We evaluate algorithms using the copycat agent scenario: a main agent is solving a set of unknown tasks $(\theta_i)_{i=0}^K$ and switches from task to task at unknown change points $(t_i)_{i=0}^K$. We denote $\theta_t^* = \sum_i \theta_i 1_{t_i \leq t < t_{i+1}}(t)$ the task being solved over time. Our goal is to construct a copycat agent predicting the main agent's tasks online through the observation of the generated state action $(s_t, a_t) \in \mathcal{S} \times \mathcal{A}$. This scenario has many different real life applications: Users of any website can be viewed as optimal agents solving iteratively a set of tasks (listening to sets of music genre, looking for different types of clothes, ..). The state space corresponds to the different web-pages and the action space is the set of buttons available to the user. We argue that predicting the task being solved online is an important feature for behaviour forecasting and content recommendation.

In the following let $x_t = (s_t, a_t)$ denote the observations and let π_θ^* denote the optimal policy of \mathcal{M}_θ . The copycat problem is a QCD problem where the observations are drawn from $f_\theta(x_{t+1}|x_t) = \mathcal{P}(s_{t+1}|s_t, a_t) \pi_\theta^*(a_{t+1}|s_{t+1})$. However this implies that we have the optimal policy π_θ^* . In practice it is sufficient to either have access to the reward functions \mathcal{R}_θ or a set of task labelled observations. In both cases the problem of learning π_θ^* is well studied. When \mathcal{R}_θ is known, then coupling Hindsight Experience Replay [2] with state of the art RL algorithms such as Soft Actor Critic [9] can solve a wide range of challenging multi-task problems [25]. When a history of observations are available, we can use generative adversarial inverse reinforcement learning [11] or Maximum Entropy Inverse Reinforcement Learning [7, 41] to learn π_θ^* .

We evaluate our algorithm performances on the *FetchReach* environment from the *gym* library. Each time the main agent achieves the desired goal, a new task is sampled. We run this experiment for 500 time step. Temporal Weight Redistribution (TWR) is used in order to evaluate the tasks online. Algorithm 1 is easily adapted to the multiple change point setting: each time a change point is detected, we reinitialise the parameters Δ and p_0 and we set the task parameters to the previous post change parameters. As such, we use the running estimate θ_0^t overtime to approximate the main agent task θ_t^* . Experimental results are reported in Figure 7.

We used the TWR algorithm with an annealing parameter $\epsilon = 0.1$ and a penalisation coefficient $c = 0.01$, and the CUSUM statistic with a cutting threshold $B_\alpha = 50$. We designate the task change points of the main agent with dashed black lines and the detected change points with a dashed red lines. On Figure 7a, we observe that the log-likelihood ratio (LLR) $\log(f_{\theta_1^t}/f_{\theta_0^t})(x_t)$ starts

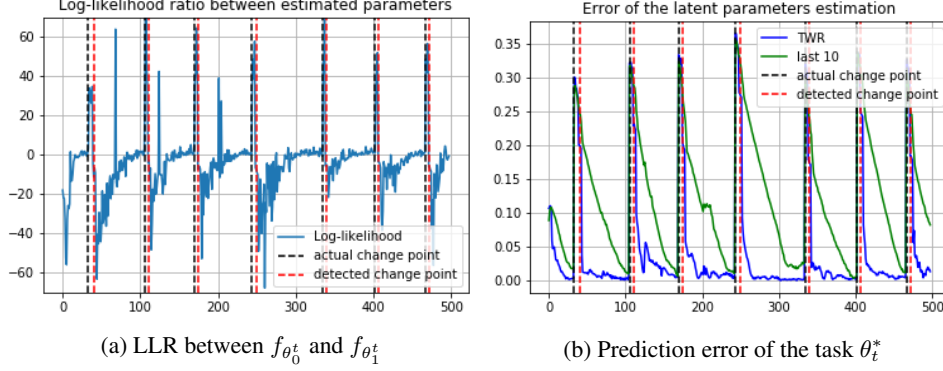


Figure 7: Performance analysis of the copycat problem

off negative, stabilises around 0 and becomes strictly positive after the actual change point. Once the change detected, we reset the TWR and the LLR falls down to a negative value. This trend is consistently reproduced with each new task. The main agent have a small probability of making a random action, this causes the LLR to peak sometimes before the change point. However this doesn't cause the statistic to exceed the threshold B_α . We provide on Figure 7b the estimation error of θ_t^* . The blue curve is the error of the TWR estimate $\|\theta_0^t - \theta_t^*\|$. As a baseline we estimate the task using the last 10 observation: $\hat{\theta}_t = \operatorname{argmax}_\theta \sum_{i=1}^{10} \log(f_\theta(x_{t-i}))$. The error of this estimator $\|\hat{\theta}_t - \theta_t^*\|$ is plotted in green. The prediction of the TWR copycat agent are clearly more reliable. Additional experimental results for the *Fetchpush* and the *PickAndPlace* environments as well as an analysis of the impact of using learned policies when solving the copycat problem are provided in the appendix.

Shared behaviours

When different tasks are associated to a shared behavior, it becomes difficult to evaluate the parameter θ_t^* . This is true for the *push* and the *PickandPlace* environments. In both cases, the goal is to control a robotic hand (through its joints' movements) in order to interact with an object until it reaches a final position (either push it there or pick it and then place it there).

The task space in these problems is the set of possible final positions. No matter what the task is, the main agent is going to reach to the object. The observations associated to this intermediate process of reaching are probably going to yield a poor estimation of the final position. However as the agent start to interact with the object, it starts to become clear what task is being executed. For this reason, an artificial change is detected between the reaching behaviour and the interaction one when using the TWR algorithm. Even though this detection is unwanted (in the sense that there was no actual change of behavior) it allows to reduce the estimation error $\|\theta_0^t - \theta_t^*\|$.

In this section, the experiment we run consists of performing three randomly sampled tasks, each over a window of 20 observations. We estimate the running task θ_t^* using the TWR algorithm and a maximum log-likelihood estimator (MLE) over both the last 5 and 10 observations. We average the errors over 500 trajectories and report the results in Figure 8. In both environments estimating the task with the running pre-change parameter of the TWR algorithm outperforms MLE. The gap grows narrower however in the *PickAndPlace* setting as the shared behaviour last longer. This makes estimations more difficult.

We also notice that the first task estimation of TWR is better than the MLE estimator despite the fact that all the observations are generated with a single parameter. This strange result is due to the detection of an artificial change after the "shared" behaviour. optimising only observations that are clearly correlated to a particular task, leads to better estimations. As for the gap in the first estimation, this is explained by a built-in agnostic behaviour in the TWR algorithm. When the number of observation is less than the **ADD** of the SHIRYAEV algorithm, the pre-change weight term $\mathbb{P}(\tau < t | \tau \sim f_n^{\theta_0^t, \theta_1^t})$ of \mathcal{L}_0^n is extremely small. and thus the estimation remains close to the initialisation. In addition, the tow target functions \mathcal{L}_0^t and \mathcal{L}_1^t are adversarial as they kind of optimise the opposite of each other. This leads to smaller gradient updates. On the other hand, MLE tend to

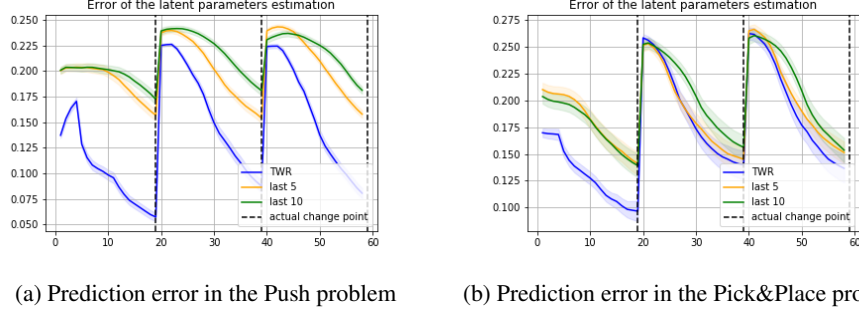


Figure 8: Performance analysis of the copycat problem

commit to a particular estimate using observations from the ‘shared’ behaviour phase. This leads generally to a heavily over-fitting estimate.

The agnostic behaviour is more pronounced in Figure 8b (*PickAndPlace*) as the robotic hand picks the object exactly the same way no matter what task is being solved. As long as there is few evidence of a distinctive behaviour occurring, the TWR estimate remains close to the initialisation. In fact the tasks here are positions and the error is the distance between the true and predicted coordinates. In the *PickAndPlace* scenario, the target is randomly sampled in a cube of edge length 0.3, in the *Push* scenario, it is sampled in a square with the same edge length. with random initialisation we get an average error of $0.1 \times \sqrt{3}$ and $0.1 \times \sqrt{2}$ respectively with a random initialisation. This coincide with the TWR error (blue curve) in both environments given few observations proving that the learned task remained close to the initialisation.

In Figure 8a, the improvement due to the artificial detection of change between the shared behaviour and the task specific one is marked around the 5th observation. In fact once the robotic hand starts pushing the object in a particular way, the estimation error starts to decay faster.

Performance cost of learning the policy

Estimating the running task θ_t^* in the copycat problem with either the TWR algorithm or the MLE requires access to the probability distribution π_θ^* . However, in real life situations, we can only learn an approximation of this distribution through historical observations.

In this section we evaluate experimentally the impact of using inverse reinforcement learning to construct an approximate policy $\hat{\pi}_\theta$ and using it as a substitute for π_θ^* . We consider the *Reach* environment where the task is to move the robotic hand to a particular position. The main agent execute 5 different tasks, sampled randomly, each over a window of 20 time steps. We evaluate the running task with TWR and MLE using the last 5 observations using the actual policy π_θ^* and the learned one $\hat{\pi}_\theta$. We average the estimation error over 100 simulations and we provide the experimental results in Figure 9. The approximate policy is constructed using the GAIL algorithm and a data-set of task labelled observations generated using π_θ^* .

As established before, the TWR estimates using the true policy (in blue) outperform MLE based approaches. This trends remains true on average when using $\hat{\pi}_\theta$. However, the true policy based MLE (in green) converges to a better estimation in the last observations before the change point, while the GAIL based TWR estimate (in red) as well as the GAIL based MLE (in orange) seem to be unable to improve. This is the cost of using a policy approximation. The additional error is built in due to estimation error of the learned policy.

E.3 Complementary performance analysis

In this section we provide complementary experimental results to the ones introduced in the paper. We keep using the same hyper-parameters (*i.e.* $\mathcal{X} = \mathbb{R}^{10}$, $\Theta = \mathbb{R}^{10}$, and (ϕ_μ, ϕ_σ) are 5-layer deep, 32-neurons wide neural network).

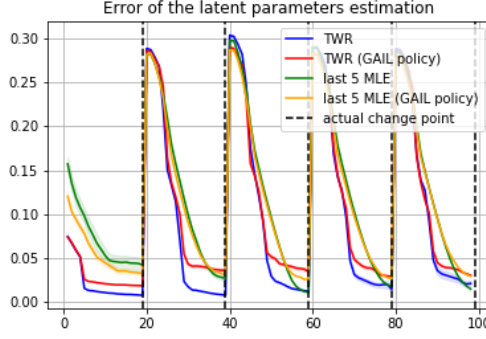


Figure 9: Impact of learning the policy

Single change point performance

In Figure 10, we provide the average regret over 500 simulations in both the BAYESIAN (on the left) and the MIN-MAX (on the right) settings. Each simulated trajectory is 1000 observation long with a change point at the 500th observation. We use the full pipeline of our algorithm with a penalisation coefficient ($c = 0.01$), and we allow the adaptive algorithm to exploit 10% of the pre change observations. Our algorithm (the blue curve) achieves comparable performance to the GLR statistic (without requiring intensive computational resources) and achieves better and more stable results compared to the adaptive algorithm (without requiring domain knowledge).

In all experiments and for all considered change detection algorithms, we observe a spike and a high variance of the average detection delay for low cutting threshold. This is a direct consequence of the definition of B_α . In fact a low cutting threshold implies a high tolerance of the type I error. This implies that the optimal detection time is no longer a reliable estimate.

Multiple change points performance

We reconsider in this section the multiple change points problem introduced early on in the paper. If the change points are sufficiently separated (i.e. $t_k - t_{k-1}$ is big enough), they can be seen as independent single change point problems. However there is no good reason to believe that this is the case of real life applications. For this reason, the detection delay of the first change point t_1 will probably reduce the accuracy at which we estimate the parameter θ_1 , this in turn will affect the accuracy of estimating the log-likelihood for the next change point t_2 . This behaviour will keep on snowballing until we reach a breaking point at which we will miss a change point. Some attempts to deal with this issue have been made in the past to improve the convergence rate of the GLR algorithm in order to reduce the impact of this problem [28]. These approaches remain computationally extensive and thus are not considered in our comparison setting.

We provide however an analysis of the impact of the number of pre change observations on the average detection delay in the single change point setting. We keep using the same hyper-parameters where $\mathcal{X} = \mathbb{R}^{10}$, $\Theta = \mathbb{R}^{10}$, and (ϕ_μ, ϕ_σ) are 5-layer deep, 32-neurons wide neural network. We use parameters achieving a KL divergence of 1.5 between the pre and post change parameters, and evaluate the average detection delay over 500 simulations where $t_2 = \lambda + 250$. By varying λ we simulate different multiple change point scenarios where the accumulated delay exhausts most of the available observations. The first thing to notice is that our algorithms (in the blue curve) has similar average detection delay to the GLR (green curve) in all presented cases. When we have sufficient observations ($\lambda = 250$), all algorithms will have reasonable performances compared to the optimal delay. However, for smaller horizon, the adaptive algorithm (the orange curve) is predicting change way before the optimal algorithm. This is explained with the bad estimation of the pre change distribution due to a reduced sample size. In fact for cutting threshold up to 10^{25} , the adaptive algorithm is predicting the change point before it happens. In addition, we observe that our approach varies less than the adaptive one as it's less prone to fit statistical fluctuations.

We provide an analysis of the impact of the number of pre change observations on the average detection delay in both the BAYESIAN (on the left) and the MIN-MAX (on the right) settings. We use parameters achieving a KL divergence of 1.5 between the pre and post change parameters, and evaluate the average detection delay over 500 simulations where $t_2 = \lambda + 250$. By varying λ we simulate different multiple change point scenarios where the accumulated delay exhausts most of the available observations. There is no notable variation in the algorithms behaviour when using either the SHIRYAEV or the CUSUM statistic. As for the impact of the number of available pre-change observation before the change point (λ), the results presented in Figure 11 illustrate how our algorithm is less prone than adaptive procedures to over fit the observation when their number is limited. In fact the blue curve (our algorithm) is closer than the adaptive one (orange curve) to the GLR (green curve) performances. All approaches end up having a constant regret with respect to the optimal detection given enough observations ($\lambda = 250$).

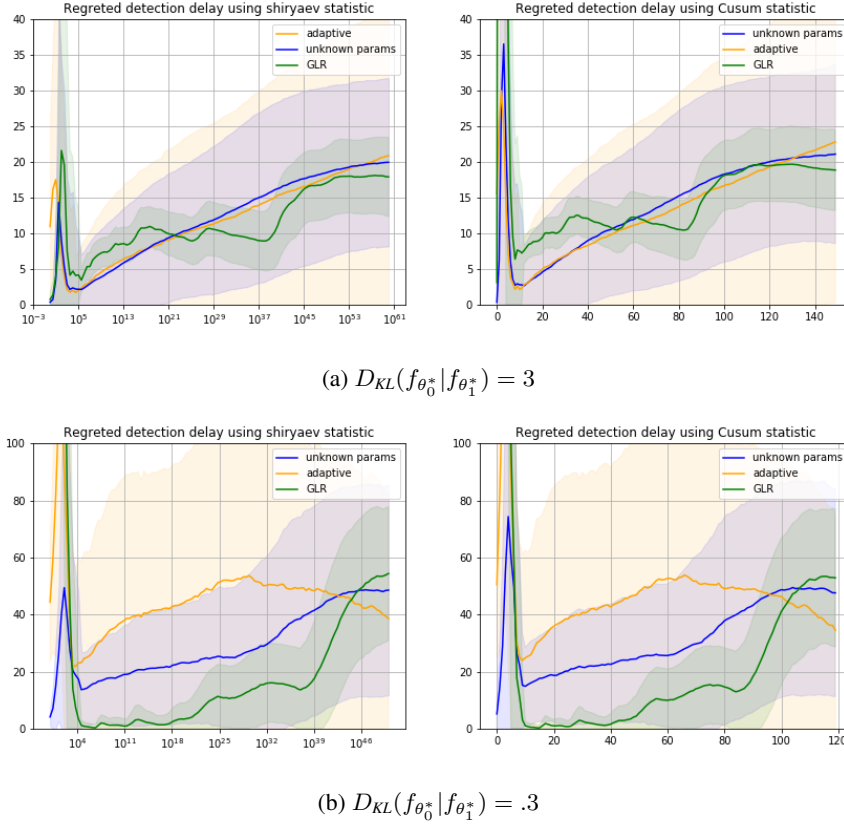
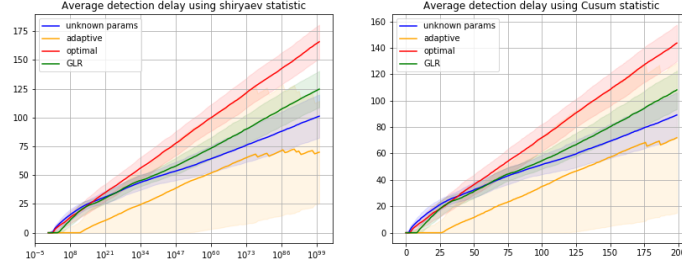


Figure 10: Performance analysis of the regretted detection delay as a function of the cutting threshold

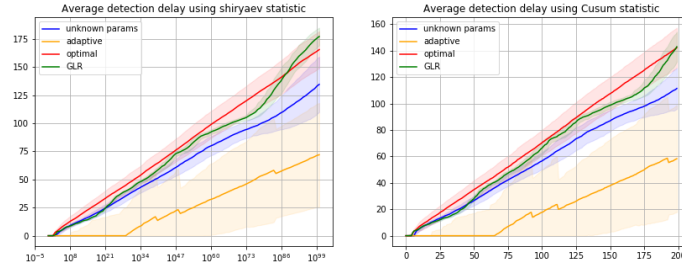
Performance given a nominal behaviour

In this section, we keep using the same hyper-parameters from the previous experiments. However we consider the setting where we have access to the pre-change parameter (which correspond to a nominal behaviour). Beside the **ADD** of the GLR and TWR statistics (computed with no prior knowledge of the pre-change parameter), we computed the **ADD** of the adaptive and TWR statistics using the prior knowledge of the true pre-change distribution.

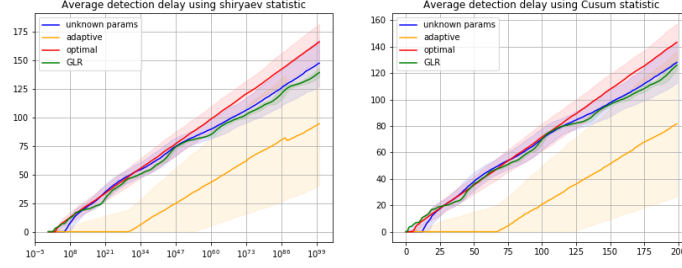
The first notable thing is that the adaptive algorithm performances (yellow curve) did not improve by much compared to the case where the parameter were estimated using 10% of the available observations. In fact TWR statistics outperforms it even with no prior knowledge of the nominal behaviour (dark blue curve). The second notable observation, is that given the pre-change parameter, TWR statistic performance (light blue) is within a constant of the GLR statistic. These observations confirm again that using the asymptotic behaviour of the Shriyaev detection delay is a very powerful approximation



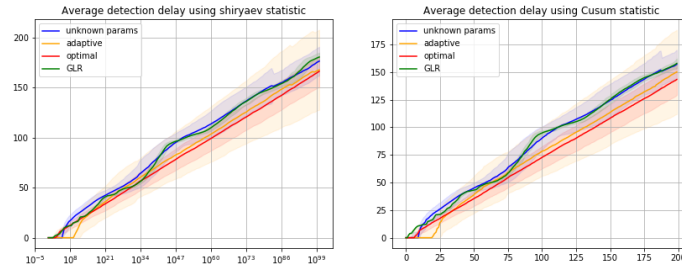
(a) $\lambda = 20$



(b) $\lambda = 50$

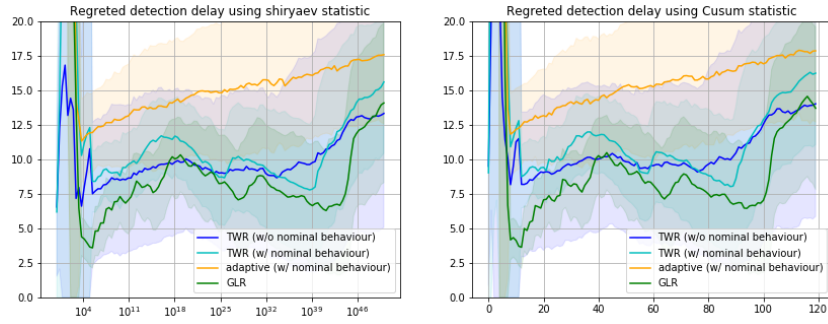


(c) $\lambda = 100$

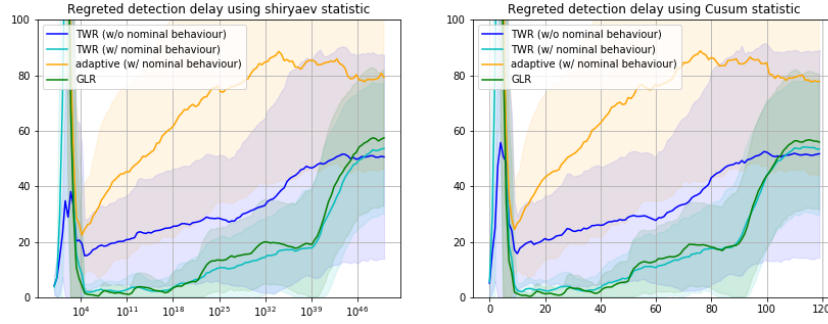


(d) $\lambda = 250$

Figure 11: Performance analysis of the average detection delay as a function of the cutting threshold



$$(a) D_{KL}(f_{\theta_0^*} | f_{\theta_1^*}) = 3$$



$$(b) D_{KL}(f_{\theta_0^*} | f_{\theta_1^*}) = .3$$

Figure 12: Performance analysis of the regretted detection delay given a nominal behaviour